The Plant Journal (2005) **43**, 29–46 doi: 10.1111/j.1365-313X.2005.02426.x

AUXIN RESPONSE FACTOR 2 (ARF2): a pleiotropic developmental regulator

Yoko Okushima[†], Irina Mitina, Hong L. Quach and Athanasios Theologis[*]
Plant Gene Expression Center, 800 Buchanan Street, Albany, CA 94710, USA

Received 7 February 2005; revised 22 March 2005; accepted 5 April 2005.
[*]For correspondence (fax 510 559 5678; e-mail theo@nature.berkeley.edu).
[†]Present address: Nara Institute of Science and Technology, Takayama 8916-5, Ikoma, Nara 630-0101, Japan.
This manuscript is dedicated to Tony Bleecker who left us too soon.

Summary

AUXIN RESPONSE FACTORS (ARFs) regulate auxin-mediated transcriptional activation/repression. They are encoded by a gene family in Arabidopsis, and each member is thought to play a central role in various auxin-mediated developmental processes. We have characterized three *arf2* mutant alleles, *arf2-6*, *arf2-7* and *arf2-8*. The mutants exhibit pleiotropic developmental phenotypes, including large, dark green rosette leaves, delayed flowering, thick and long inflorescence, abnormal flower morphology and sterility in early formed flowers, large organ size and delayed senescence and abscission, compared with wild-type plants. In addition, *arf2* mutant seedlings have elongated hypocotyls with enlarged cotyledons under various light conditions. The transcription of *ACS2*, *ACS6* and *ACS8* genes is impaired in the developing siliques of *arf2-6*. The phenotypes of all three alleles are similar to those of the loss-of-function mutants obtained by RNA interference or co-suppression. There is no significant effect of the mutation on global auxin-regulated gene expression in young seedlings, suggesting that ARF2 does not participate in auxin signaling at that particular developmental stage of the plant life cycle. Because ARF2 is thought to function as a transcriptional repressor, the prospect arises that its pleiotropic effects may be mediated by negatively modulating the transcription of downstream genes in signaling pathways that are involved in cell growth and senescence.

Keywords: growth, senescence, auxin response factor, ACC synthase.

Introduction

The plant hormone auxin typified by indole-3-acetic acid (IAA) regulates a variety of physiological and developmental processes, including apical dominance, tropic responses, lateral root formation, vascular differentiation, embryo patterning and shoot elongation (Davies, 1995). At the cellular level, auxin application modulates cell elongation, division and differentiation through transcriptional regulation of specific genes (Abel and Theologis, 1996; Leyser, 2002). Two classes of transcription factors, ARF and the Aux/IAA proteins, act as the key regulators of auxin-mediated gene expression (Guilfoyle *et al.*, 1998; Liscum and Reed, 2002). A typical ARF protein contains a B3-like DNA binding domain in its N-terminus region and domains III and IV similar to those present in the Aux/IAAs in their C-terminus region (Guilfoyle and Hagen, 2001; Ulmasov *et al.*, 1997b). The ARF proteins bind to auxin-responsive elements (*AuxREs*) in the promoter region of auxin-responsive genes, including *Aux/IAAs*, through their DNA binding domain (Abel *et al.*, 1996; Ulmasov *et al.*, 1997b, 1999a). The amino acid composition of their middle region determines whether an ARF protein is a transcriptional activator or repressor (Tiwari *et al.*, 2003; Ulmasov *et al.*, 1999b). The Aux/IAAs are short-lived nuclear proteins; most of them contain four highly conserved domains (I–IV) (Abel *et al.*, 1994; Reed, 2001). Each domain contributes to the functional properties of the protein (Kim *et al.*, 1997; Ouellet *et al.*, 2001; Ramos *et al.*, 2001; Tiwari *et al.*, 2004; Ulmasov *et al.*, 1997b, 1999a). The Aux/IAA proteins, while they do not bind to the *AuxRE*s directly, regulate auxin-mediated gene expression by controlling the activity of ARFs by protein–protein interactions (Kim *et al.*, 1997; Tiwari *et al.*, 2003; Ulmasov *et al.*, 1997b). These molecular observations suggest that the vast and diverse combinations of dimers among the Aux/IAA and ARF gene family members may regulate auxin-mediated gene

expression in a cell- and tissue-specific manner (Abel *et al.*, 1994; Kim *et al.*, 1997). The prospect arises that auxin signals are converted into specific responses by matching pairs of co-expressed ARF and Aux/IAA proteins (Weijers and Jurgens, 2004). More importantly, the Aux/IAA proteins are targets for degradation by the SCF^{TIR1} complex, and auxin promotes directly the interaction of Aux/IAAs with the SCF^{TIR1} complex (Dharmasiri and Estelle, 2004; Gray *et al.*, 2001). Therefore, stability of the Aux/IAA proteins is the central regulator of auxin signaling.

Several gain-of-function Aux/IAA mutants, including *shy2/iaa3* (Tian and Reed, 1999), *axr2/iaa7* (Nagpal *et al.*, 2000), *slr/iaa14* (Fukaki *et al.*, 2002), *arx3/iaa17* (Rouse *et al.*, 1998) and *iaa28-1* (Rogg *et al.*, 2001) and *axr5/iaa1* (Yang *et al.*, 2004), have been isolated by forward genetics. These mutants have amino acid substitutions in highly conserved residues of domain II, and they cause altered auxin response and dramatic defects in growth and development. Loss-of-function mutations of *AUX/IAA*s do not show an obvious visible growth phenotype (Nagpal *et al.*, 2000; Rouse *et al.*, 1998; Tian and Reed, 1999; Y. Okushima and A. Theologis, unpublished data). Forward and reverse genetic analyses led to the isolation of loss-of-function mutants in five *ARF* genes. Mutations in *ARF3/ETT* affect gynoecium patterning (Nemhauser *et al.*, 2000; Sessions *et al.*, 1997). Loss-of-function mutations of *ARF7/NPH4/MSG1* result in impaired hypocotyl response to blue light and other differential growth responses associated with changes in auxin (Harper *et al.*, 2000; Stowe-Evans *et al.*, 1998; Watahiki and Yamamoto, 1997). Mutations in *ARF5/MP* interfere with the formation of vascular strands and the initiation of the body axis in the early embryo (Hardtke and Berleth, 1998). Mutations in *ARF2/HSS* have been identified as extragenic suppressors of the hookless phenotype. It appears that *ARF2* acts as one of the communicating links between the ethylene signaling pathway and other signaling pathways for regulating apical hook formation (Li *et al.*, 2004). Lastly, *ARF8* functions in hypocotyl elongation and is involved in auxin homeostasis (Tian *et al.*, 2004).

Functional genetic analysis of the *ARF* gene family members using reverse genetic analysis led to the identification of T-DNA insertions in 18 of the 23 *ARF* genes (Okushima *et al.*, 2005). Most of the mutants failed to show an obvious growth phenotype, except for the previously identified mutants mentioned above, suggesting that there are functional redundancies among the ARF proteins. Subsequent construction of double mutants among the various *ARF* single mutants led to identification of several double mutants with novel and unique developmental defects. For example, the *arf7 arf19* double mutant shows severe auxin-related phenotypes not found in the *arf7* and *arf19* single mutants, including severely impaired lateral root formation and abnormal gravitropism in the hypocotyl and the root (Okushima *et al.*, 2005). The phenotype of *arf1arf2* (Li *et al.*, 2004; Okushima *et al.*, 2005) is similar to, but much stronger than, that of *arf2* reported by Li *et al.* (2004), and *ar6arf8* has dwarfed aerial tissue and exhibits severe defects in flower development (Okushima *et al.*, 2005). The analysis suggests the presence of both unique and overlapping functions among the *ARF* gene family members in Arabidopsis (Okushima *et al.*, 2005).

Herein, we report the phenotypic characterization of three *arf2* insertion mutants identified during the global functional analysis of the *ARF* gene family members (Okushima *et al.*, 2005). All the mutants show the same developmental defects including large leaf size and inflorescence stem, flowers with abnormal morphology, delayed flowering and senescence. In addition, *arf2* seedlings have long hypocotyls under various light conditions. Null mutant transgenic lines obtained by co-suppression and RNA interference (RNAi) have the same phenotypes as the T-DNA alleles. The data suggests that ARF2 is a part of transcriptional complexes responsible for regulating diverse signaling pathways leading to pleiotropic developmental defects.

Results

The ARF2 *gene and its insertions*

Figure 1(a) shows the structure of the *ARF2* gene and the location of three T-DNA insertion alleles, *arf2-6*, *arf2-7* and *arf2-8*, previously reported by Okushima *et al.* (2005). The *ARF2* gene (At5g62000) has 15 exons and encodes a 95.7-kDa polypeptide (v5.0 of the Arabidopsis genome annotation, Okushima *et al.*, 2005). The At5g62000 locus was originally annotated to contain two open reading frames (ORFs) adjacent to each other (The Arabidopsis Genome Initiative, 2000). One ORF was annotated as 'auxin response factor-like protein' (At5g62000) and the other as 'ARF1 binding protein' (At5g62010), as noted by Li *et al.* (2004). Isolation of full-length cDNAs (AF378862, AY669787) showed these two ORFs to be part of a single gene named *AUXIN RESPONSE FACTOR 2* (*ARF2*) (Ulmasov *et al.*, 1999b). The T-DNA insertions of *arf2-6* and *arf2-8* are located in the 12th exon, after codon G494 (nt T2549 from ATG) and N677 (nt C3097), respectively. The insertion of *arf2-7* is located in the 13th exon after codon F768 (nt G3962). All three insertions are located downstream of the DNA binding domain of ARF2 (Figure 1a). RT-PCR analysis using primers annealing to the 3′ region of *ARF2* (primers F2 and R2; Figure 1a), detected no expression downstream of the *arf2-6* and *arf2-7* insertions (Figure 1b, top panel). However, similar analysis with primers annealing to the 5′ region of *ARF2* upstream of the insertions (F1 and R1; Figure 1a) detected the expression of truncated *ARF2* transcripts in higher abundance than that of the intact wild-type transcript (Figure 1b). The expression of the *ARF2* mRNA in wild type and *arf2-6* allele was also determined in

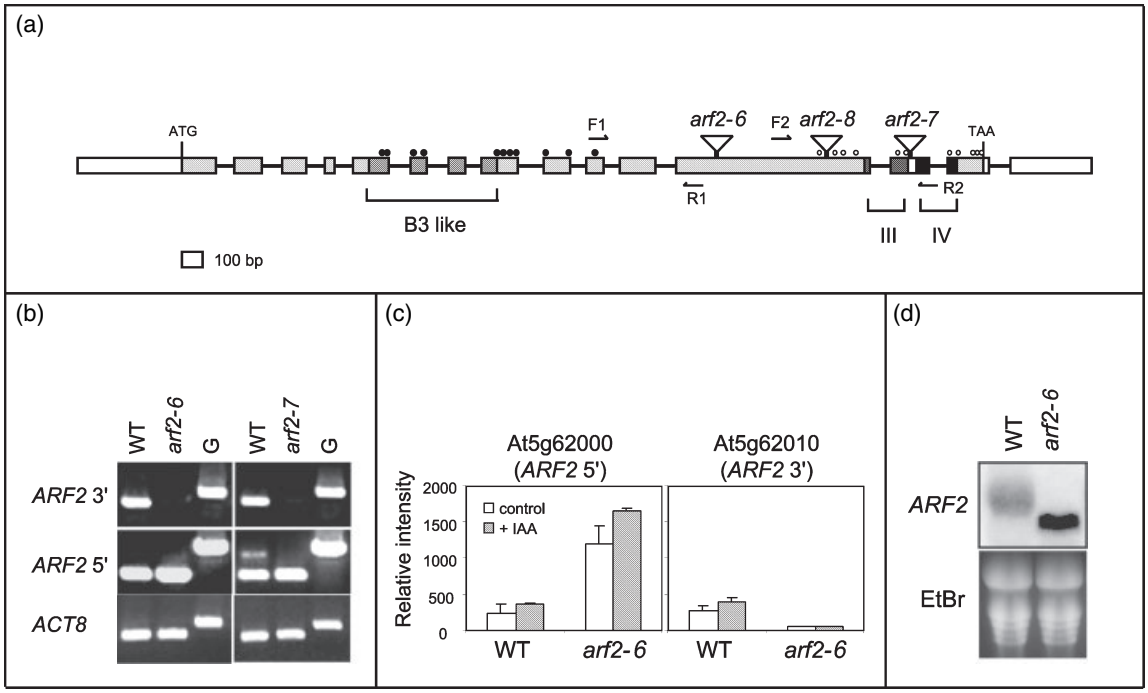

Figure 1. *ARF2* T-DNA insertion mutants.
(a) Structure of the *ARF2* gene and locations of the T-DNA insertions. Boxes and lines represent exons and introns, respectively. The locations of ATG and TAA codons are indicated. White boxes represent the 5′ and 3′-UTRs and gray boxes represent coding regions respectively. The conserved B3-like DNA binding domain, domains III and IV among the various ARFs, are also shown. The T-DNA insertions in the three different mutant alleles are marked by open triangles and the corresponding allele is shown above the triangle. Arrows indicate positions of primers used for RT-PCR analysis. The positions of 11 oligonucleotide probes on the Affymetrix ATH1 GeneChip are indicated by small closed (corresponding to the annotated gene At5g62000) and open (corresponding to the previously annotated gene At5g62010; it was recently re-annotated being part of At5g62000) circles.
(b) Detection of *ARF2* transcripts by RT-PCR in *arf2-6*, *arf2-7* mutant seedlings and their segregated parental wild type (WT). PCR primers spanning introns were used to distinguish between amplification of cDNA and genomic DNA (lane G). The expression of *ACT8* gene was used as a control.
(c) Expression profiles of the 5′-region of (left, At5g62000) and 3′-region (right, At5g62010) of the *ARF2* gene derived from Affymetrix ATH1 GeneChip data. The data represent the average relative intensity expression levels of control (open bar) or auxin-treated samples (gray bar) from triplicate experiments.
(d) RNA hybridization analysis of *ARF2* expression in WT and *arf2-6* mutant seedlings. Each lane contains 20 μg total RNA. Ethidium bromide staining of the agarose gel is shown as a loading control (lower panel; see Experimental procedures for experimental details).

this study from experiments on the effect of *arf2-6* mutation on global auxin-regulated gene expression using high-density oligonucleotide arrays (Affymetrix ATH1 GeneChip; see below). The Affymetrix ATH1 GeneChip was originally designed according to the annotation of the Arabidopsis Genome Initiative (2000) and thus has two probe sets; one set corresponds to At5g62000 (5′ region of *ARF2*) and the other to At5g62010 (3′ region of *ARF2*). All the probes upstream of the insertions are part of the At5g62000 probe set whereas all probes downstream of the insertions are part of the At5g62010 probe set (Figure 1a). Therefore, the relative intensity of the At5g62000 probe set will represent the *ARF2* expression level upstream of the *arf2-6* insertion and the relative intensity of the At5g62010 probe set will reflect the *ARF2* expression level downstream of the *arf2-6* insertion. The results shown in Figure 1(c) indicate that *ARF2* expression in wild-type seedlings, which is represented by the relative intensities of both At5g62000 (control: 232.2 ± 121.5; IAA-treated: 368.2 ± 7.1) and At5g62010 (control: 272.2 ± 66.2; IAA-treated: 394.3 ± 53.3), is very similar and slightly induced by IAA treatment. In the *arf2-6* mutant, the relative intensity of At5g62010, which reflects the expression level of the 3′ *ARF2* mRNA, is the same as the background level of intensity (control: 50.0 ± 0; IAA-treated: 50.0 ± 0). This is in agreement with the RT-PCR analysis shown in Figure 1(b). In contrast, enhanced expression of the 5′ *ARF2* mRNA is detected in the *arf2-6* mutant compared with the wild type (control: 1205.4 ± 245.6; IAA-treated: 1649.5 ± 35.6). These results indicate that the truncated *ARF2* mRNA is highly expressed in the *arf2-6* mutant. These results were also confirmed by RNA hybridization analysis (Figure 1d). The increased level of the *arf2-6* truncated transcript is attributed to an enhancement of RNA stability. The *arf2-6* allele has been preferentially used for detailed phenotypic analysis (described below) because it has the most upstream T-DNA insertion among the three insertions. The *arf2-8* allele is the most recently identified among the three alleles, and has been less characterized than the other alleles. However, all three *arf2* T-DNA insertion mutants display the same

major phenotypic aberrations (Figure 5 below provides a phenotypic and molecular comparison of all *arf2* alleles together with the Pro_{35S}:*ARF2* and RNAi lines).

Expression patterns of ARF2

The *arf2* T-DNA insertion mutants have several morphological defects during the course of Arabidopsis development (see below). This suggests that *ARF2* expression may be ubiquitous throughout development. Previous studies by Ulmasov *et al.* (1999a) have shown that *ARF2* is expressed in all major plant organs including roots, rosette and caulin leaves, flowers and siliques. These expression characteristics were also confirmed by us using RT-PCR analysis (data not shown). We also generated transgenic plants expressing Pro_{ARF2}:*GUS* in order to monitor *ARF2* expression during development. GUS activity was detected in the peripheral zone of cotyledons and in the bottom region of the hypocotyl and in the root vasculature in 3-day-old, light-grown transgenic seedlings (Figure 2a). However, little or no GUS expression was detected in cotyledons of etiolated seedlings. Strong staining was detected in hypocotyls, especially in the shoot apex region of etiolated seedlings. Expression of Pro_{ARF2}:*GUS* was detected in the vascular tissue and the initiation sites of lateral roots (Figure 2a, insert). High expression levels of Pro_{ARF2}:*GUS* were detected in the sepals and stamen as well as in the apices and bases of pistils (Figure 2b–g). Pro_{ARF2}:*GUS* was also expressed in developing siliques and seeds (Figure 2h).

Pleiotropic morphological phenotypes in arf2 *mutants*

Young *arf2-6* seedlings (4–5 days old) are phenotypically almost indistinguishable compared with the wild-type seedlings grown under normal growth chamber conditions (16 h white light/8 h dark cycle). Etiolated *arf2-6* and *arf2-7* seedlings exhibit the normal tropic responses of the wild-type seedlings (data not shown). Their phenotype remains the same until the late vegetative phase except for small differences noticed in cotyledon and hypocotyl size. *arf2-6* plants have slightly enlarged cotyledons and elongated hypocotyls compared with the wild type (data not shown). These phenotypes are affected by light conditions (see below). The morphological phenotype of *arf2* mutants becomes obvious after they enter the state of reproductive development. Homozygous plants of the *arf2-6, arf2-7* and *arf2-8* have flowers with altered morphology (Figure 3a–e), large and dark green rosette leaves (Figure 3f), and long and thick inflorescence stems compared with those of wild-type plants (Figure 3h). In order to establish that the phenotypes of *arf2* mutants were caused by the T-DNA insertions in the *ARF2* gene locus, we examined the linkage between mutant phenotype and T-DNA insertion. Homozygous mutant plants *arf2-6/arf2-6* or *arf2-7/arf2-7* were backcrossed to wild-type Col and the phenotypes of the F_2 progeny were analyzed. Among the F_2 plants [$n = 67$ (*arf2-6*) and $n = 63$ (*arf2-7*)], only homozygous plants for the insertion (*arf2-6/arf2-6* or *arf2-7/arf2-7*) have the abnormal flower phenotype.

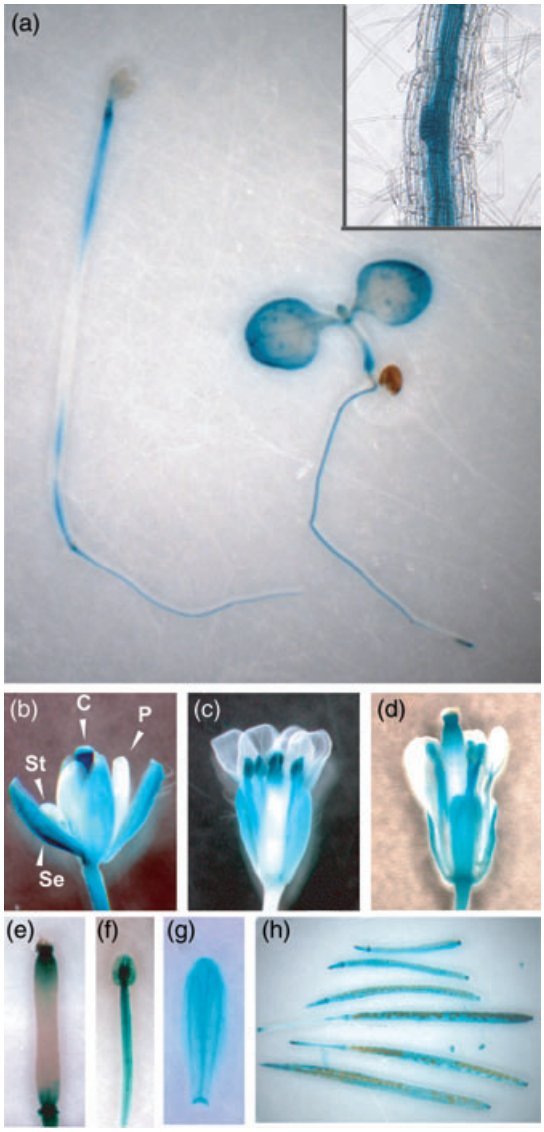

Figure 2. Expression of *ARF2* promoter-GUS fusion in transgenic plants.
(a) GUS staining patterns in etiolated (left) and light-grown (right) Pro_{ARF2}:*GUS* transgenic seedlings (3-day old). Enlarged root vascular region displaying lateral root primodium with GUS staining is shown in the inset.
(b) GUS activity in the flower bud of the Pro_{ARF2}: *GUS* plant. The sample was pushed and squashed out to show each floral organ. Arrowheads indicate carpel (C), stamen (St), sepal (Se) and petal (P).
(c) GUS staining patterns in the flower of Pro_{ARF2}:*GUS* plant just after anthesis.
(d) GUS staining patterns in the flower of Pro_{ARF2}:*GUS* plant at a stage slightly later than that shown in (c).
(e) Pro_{ARF2}:*GUS* expression in pistil.
(f) Pro_{ARF2}:*GUS* expression in stamen.
(g) Pro_{ARF2}:*GUS* expression in sepal.
(h) Pro_{ARF2}:*GUS* expression in developing siliques and seeds of T_2 plants.

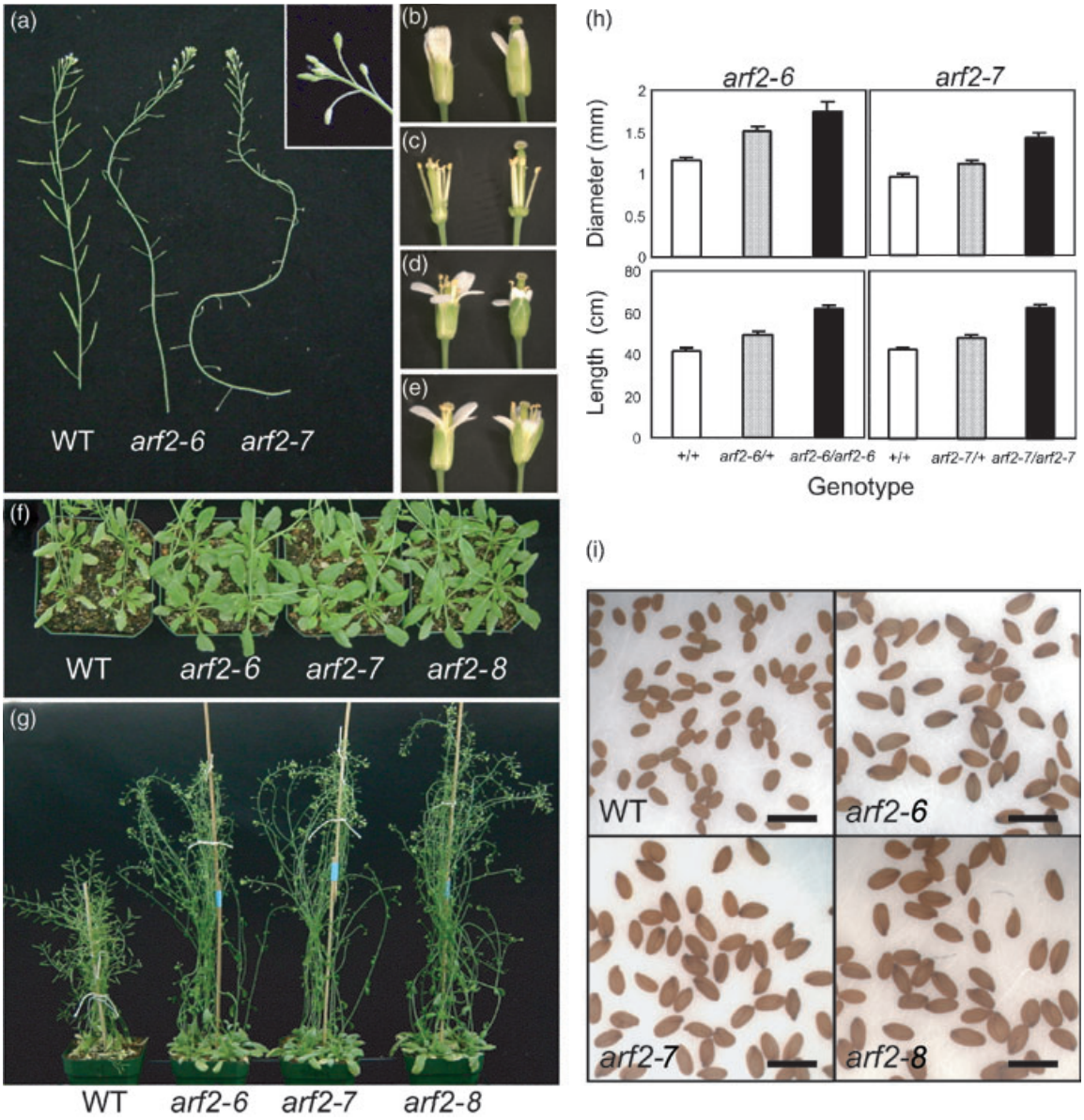

Figure 3. Morphological phenotypes of the *ARF2* T-DNA insertion mutants.
(a) Young primary inflorescence stems of wild type (WT), *arf2-6* and *arf2-7* plants. All early produced flowers of *arf2-6* and *arf2-7* mutants are sterile and siliques do not develop. Early produced flowers of *arf2-6* (unopened) are shown in the inset.
(b–e) Flower phenotype of WT (left) and *arf2-6* (right). (c) Petals and sepals were removed to show stamens and pistils of the same flowers shown in (b). Flowers shown in (d) were produced later than those shown in (b) and (c). Flowers shown in (e) were produced later than those shown in (d). Flower phenotype of *arf2* mutants became less severe as the plants grew older.
(f) Rosette leaves of 6-week-old WT, *arf2-6*, *arf2-7* and *arf2-8* plants. Leaf size in mm^2 ($n = 4$): WT, 174; *arf2-6*, 387; *arf2-7*, 361; arf2-8, 344.
(g) Eight-week-old WT, *arf2-6*, *arf2-7* and *arf2-8* plants. Each pot contains four plants.
(h) Diameter (top) and length (bottom) of primary inflorescence stems of 9-week-old WT, heterozygote and homozygote *arf2-6* and *arf2-7* plants. Genotypes of approximately 70 individual F_2 plants resulting from a backcross of *arf2-6*/*arf2-6* and *arf2-7*/*arf2-7* plants with WT were determined and the average length and diameter of primary inflorescence of each genotype were then calculated. Bars represent SE of the average.
(i) Seeds of WT, *arf2-6*, *arf2-7* and *arf2-8*. Bar = 1 mm.

Wild type or heterozygous plants have flowers with normal morphology, suggesting that the abnormal flower phenotype co-segregates with the corresponding insertion in the *ARF2* gene and that the phenotype is recessive. The flower phenotype is most severe in early-formed flowers, and all of them are sterile (Figure 3a). The predominant morphological defect of the *arf2* mutant flowers is observed in the gynoecium and sepals. The flowers of *arf2* mutants have significantly elongated gynoecia and sepals, compared with the wild type (Figure 3b,c). The first formed flower buds of

arf2 mutants are tightly closed by the elongated sepals, and they never open (Figure 3a, insert). Late formed flowers can open, but still have significantly elongated sepals (Figure 3b). Furthermore, the gynoecium elongates earlier relatively to the rest of the developing flower, often protruding out of the sepals and petals (Figure 3b). As the length of stamen filaments is shorter than that of pistils in the *erf2* mutant flowers (Figure 3c,d), the anthers fail to touch the stigma. This probably causes infertility of the early produced flowers. The flower phenotypes of *arf2* mutants become less severe as the plants grow (Figure 4a,b); late-formed flowers are fertile and produce abundant amount of seeds (Figure 4a,b). These flower phenotypes are observed in all three *arf2* T-DNA insertion alleles (see Figure 5).

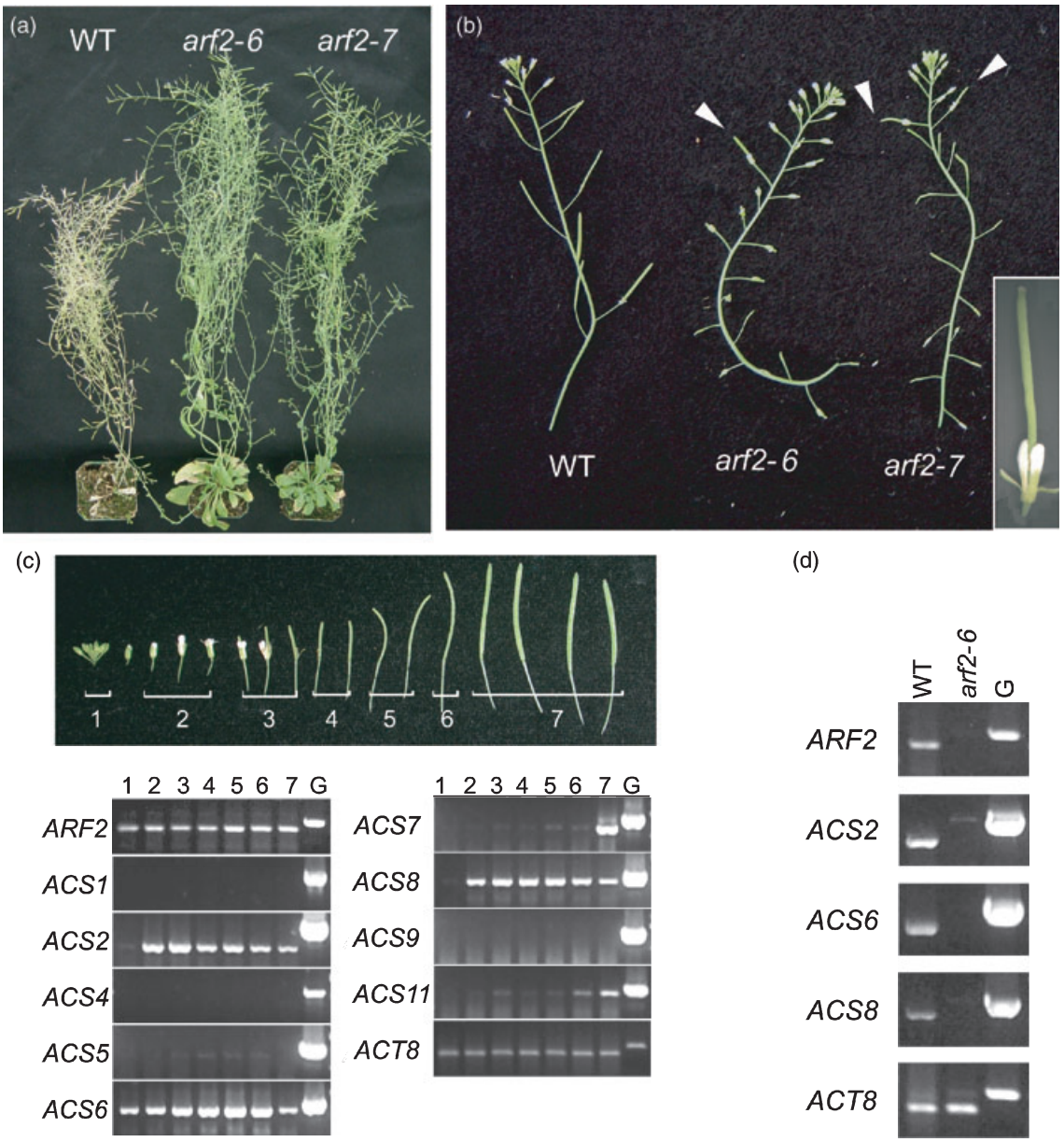

Figure 4. Delayed senescence phenotype of the *ARF2* mutants.
(a) Eleven-week-old wild type (WT), *arf2-6* and *arf2-7* plants.
(b) Inflorescence of WT, *arf2-6* and *arf2-7* plants. Arrowheads indicate developing siliques with unwithering and fresh floral organs in *arf2-6* and *arf2-7* mutants. Close up view of a long developing silique with fresh floral organ in the *arf2-6* mutant is shown in the inset.
(c) Expression of the *ACS* genes during flower and silique development in wild-type plants. The seven stages of tissue sampling for RNA extraction are shown on top (see Experimental procedures). RT-PCR was performed with cDNA, derived from the corresponding stages indicated above. G indicates genomic DNA as a control. Approximately equal amounts of *ACT8* PCR product were amplified from all samples.
(d) RT-PCR analysis of *ACS2*, *ACS6* and *ACS8* genes in flowers (just after anthesis) of WT and *arf2-6* mutant.

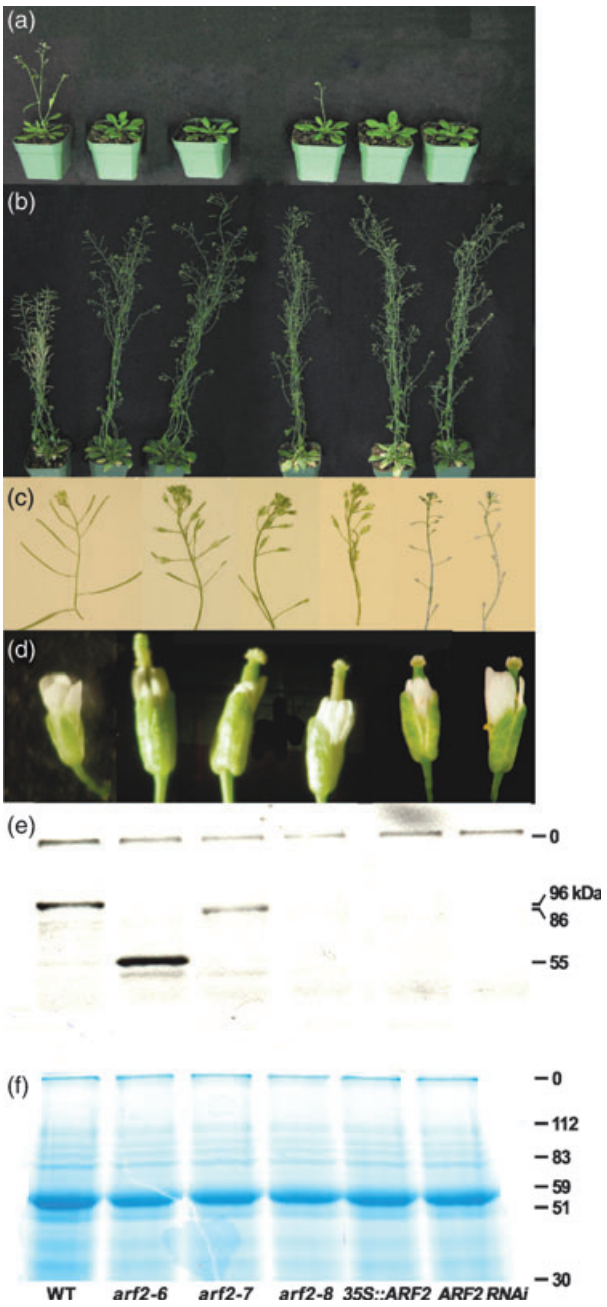

Figure 5. Phenotypic comparison of the *arf2* mutants, *ARF2* overexpressor and *ARF2-RNAi*.
(a) Thirty-five-day-old plants.
(b) Sixty-three-day-old plants.
(c) Infloresence of 56-day-old plants.
(d) Flowers.
(e) Expression of the ARF2 protein determined by Western analysis. The sizes of the truncated polypeptides are: ARF2, 96; arf2-6, 55; arf2-7, 86; arf2-8, 75 kDa (see Experimental procedures for technical details).
(f) Portion of the protein-stained gel used for Western analysis. The various mutants and transgenic lines shown on each panel are indicated at the bottom of the figure.

In addition to the flower phenotype, *arf2* mutant plants are larger in size than the wild-type plants (Figure 3g). We noticed some variability in the rate of growth among the three alleles which is independent of the allele type. The final height of all alleles is approximately the same. Moreover, all three *arf2* alleles have enlarged rosette leaves (Figure 3f) and long inflorescence stems (Figure 3g,h). The average length of the primary inflorescence stems of homozygous *arf2-6* (*arf2-6/arf2-6*) and *arf2-7* (*arf2-7/arf2-7*) mutant plants is significantly longer than that observed in wild-type plants (Figure 3h). Likewise, the average diameter of the primary inflorescence stems of homozygous *arf2-6* (*arf2-6/arf2-6*) and *arf2-7* (*arf2-7/arf2-7*) mutant plants is also significantly greater than that observed in wild-type plants (Figure 3h). However, heterozygote *arf2-6* (*arf2-6/+)* and arf2-7 (*arf2-7/+)* mutant plants have intermediate length and thickness of inflorescence stems between those of wild type (+/+) and homozygous *arf2* (*arf 2-6/arf 2-6* and *arf 2-7/arf 2-7*) mutant plants (Figure 3h). These results suggest that *arf2* T-DNA insertion alleles are recessive with respect to flower morphology, and semidominant with respect to the length and thickness of inflorescence stems. The seeds of homozygous *arf2* mutants are larger than wild-type seeds (Figure 3i).

Delayed senescence and abscission in arf2 *mutants*

The growth of wild-type plants stops approximately 7 weeks after germination, and the plants are completely aged by day 75 from germination (Figure 4a). However, *arf2-6* and *arf2-7* mutant plants of similar age still have green rosette leaves and stems (Figure 4a). In addition, the floral organs of *arf2* mutants show delayed senescence and abscission. The early produced flowers of *arf2* mutants are infertile, but the ratio of fertile/infertile flowers increases as the plants grow (Figure 4a,b). In wild-type plants, floral organs are shed shortly after anthesis (Figure 4b,c), whereas, fresh floral organs are attached to the relatively longer developing siliques in *arf2* mutants (Figure 4b), suggesting delayed floral abscission as well as delayed senescence.

The increased resistance of the *arf2* mutants to senescence suggested that components of ethylene biosynthesis or perception may be defective. We determined the expression of the *ACS* gene family members (Yamagami *et al.*, 2003) in mutant flowers. First we performed semiquantitative RT-PCR analysis using cDNAs synthesized from total RNA isolated from developing flower and silique samples collected from seven stages, based on their morphological appearance (Figure 4c) (Okushima *et al.*, 2005). Primers spanning predicted introns were used to distinguish between amplification of genomic DNA contamination and amplification of cDNA. The data show that *ARF2* is constitutively expressed throughout flower and silique development (Figure 4c). Among the eight functional *ACS* gene family genes tested (Yamagami *et al.*, 2003), *ACS2* and *ACS8*

show similar expression profiles during flower and silique development and their expression is almost nil in unopened flower buds (stage 1), but strongly induced after anthesis (stage 2). *ACS6* is expressed in flowers and in all the silique developmental stages, but its expression level is dramatically increased by stage 6. The expression of *ACS7* appears to be dramatically induced after seed maturation (stage 7). *ACS11* shows an expression profile similar to that of *ACS7*, and may be involved in silique senescence. According to the expression analysis, it is possible that *ACS2*, *ACS6* and *ACS8* are involved in floral organ senescence and abscission. RT-PCR analysis with RNA from stage 3 flowers (Figure 4c) showed that transcription of *ACS2*, *ACS6* and *ACS8* is inhibited in flowers by the *arf2-6* mutation (Figure 4d).

ARF2 *overexpression and RNAi-based suppression*

To investigate further the function of *ARF2* during plant growth and development, we generated transgenic lines overexpressing the full-length *ARF2* ORF (P_{35S}:*ARF2*) and having the endogenous ARF2 transcript suppressed by RNAi (Wesley *et al.*, 2001). All T_1 plants ($n = 48$) transformed with P_{35S}:*ARF2* showed phenotypes similar to *arf2* T-DNA insertion mutants in the adult stage. Several lines with single insertion were selected in the T_2 generation and one T_3 homozygous line was used for further analysis. Figure 5 compares the phenotypes of young and mature plants and their flower morphology among the three *arf2* alleles, P_{35S}:*ARF2* and ARF2-RNAi lines. All mutant and transgenic lines have similar phenotypic characteristics described above, that is, large and dark green rosette leaves, delayed flowering, thick and long inflorescence, abnormal flower morphology and sterility in early generated flowers and delayed senescence and abscission (Figure 5a–d and data not shown). Western analysis with an ARF2-specific antibody indicates that the *arf2-6* mutant accumulates considerable amounts of the truncated polypeptide, in agreement with the enhanced level of the corresponding transcript (Figure 1b–d). The *arf2-7* allele accumulates small amounts of the corresponding truncated polypeptide, whereas *arf2-8* is a null (Figure 5e). The P_{35S}:*ARF2* and RNAi transgenic lines do not express any ARF2 protein. They are nulls (Figure 5e). It appears that *ARF2* overexpression results in co-suppression of the *ARF2* transcript.

Growth response of arf2 *mutants under Rc and FRc light*

Under greenhouse growth conditions (long day; 16 h light/ 8 h dark), the flowering of *arf2-6* and *arf2-7* is delayed by approximately 1 week compared with the wild type, and the mutants have more rosette leaves (Figure 6a). During our search for phenotypic abnormalities, we observed that some of the phenotypes (e.g., delayed flowering in long-day conditions, large plant size and slightly dark green leaves) have also been seen in the *gigantea* (*gi*)-*100* mutant (Huq *et al.*, 2000) grown in the greenhouse room (data not shown). Although the delayed flowering phenotype is more pronounced in *gi-100* than in *arf2* (Fowler *et al.*, 1999; Huq *et al.*, 2000; Koornneef *et al.*, 1995), the other phenotypes of *arf2*, such as defects in flower morphology, delayed abscission, are not seen in *gi-100* (data not shown). The partial phenotypic similarity between *gi-100* and *arf2* prompted us to examine the behavior of *arf2* mutants under various light conditions. We also observed that the hypocotyls of *arf2* mutant seedlings were slightly longer than the wild type under weak white light conditions. The *arf2* mutants also showed a lower germination ratio when they were kept in the dark without white light treatment following 3 days of cold treatment (4°C) in the dark (the seeds were plated on agar plates in a regular sterile hood under ordinary fluorescent light). Under these experimental conditions, approximately 50% of the *arf2-6* and *arf2-7* seeds did not germinate, whereas, almost all the wild-type seeds germinated normally (data not shown). However, when these plates were left on the bench top, all non-germinated seeds began to germinate the next day. In addition, when we treated the plates with white light for 3 h before transferring to the dark, all *arf2-6* seeds germinated. These observations suggest that the light signaling pathway(s) are impaired in the *arf2* mutants, reinforced by observations by others that many light-related mutants also show altered flowering times (Hayama and Coupland, 2004; Valverde *et al.*, 2004).

Figure 6. Light-related phenotypes of *arf2* mutants.
(a) *arf2* mutants show delayed flowering time. Flowering time of the wild type (WT) and two *arf2* insertion mutant lines, *arf2-6* and *arf2-7*, are shown. Days of bolting (open bar) and rosette leaf number (black bar) were determined when the plants bolted under long-day (18 h light/ 6 h dark) condition at 21°C. The data are expressed as average of more than 12 plants per each line. Bars represent SE of the average.
(b) Phenotype of WT, *arf2-6*, *phyA-211* and *phyB-9* mutant seedlings grown for 4 days under various light conditions: continuous white (Wc), red (Rc; 15.28 μmol m^{-2} sec^{-1}), far red (FRc; 11.98 μmol m^{-2} sec^{-1}) light and darkness.
(c) Left: Rc fluence rate–responses curve for hypocotyl length in WT, *arf2-6*, *phyA-211* and *phyB-9* seedlings. Hypocotyl length is expressed as the average of more than 25 seedlings. Bars represent SE of the average. Middle: cotyledon area of WT, *arf2-6*, *phyA-211* and *phyB-9* seedlings grown under Rc (15.28 μmol m^{-2} sec^{-1}) for 4 days. Right: the original seedling sample plate for this experiment at 15.28 μmol m^{-2} sec^{-1} Rc (as red arrow in fluence rate–response curve graph). *arf2-6* mutant seedlings showed significantly elongated hypocotyls compared with WT.
(d) Left: FRc fluence rate–response curve for hypocotyl length in WT, *arf2-6*, *phyA-211* and *phyB-9* seedlings. Hypocotyl length is expressed as the average of more than 25 seedlings. Bars represent SE of the average. Middle: cotyledon area of WT, *arf2-6*, *phyA-211* and *phyB-9* seedlings grown under FRc for 4 days. Right: the original seedling sample plate for this experiment at 0.81 μmol m^{-2} sec^{-1} FRc (shown as red arrow in fluence rate–response curve graph). *arf2-6* mutant seedlings showed significantly elongated hypocotyls similar to the *phyA-211* mutant.

We subsequently investigated the light sensitivity of *arf2* mutants under continuous red (Rc) or far-red (FRc) light conditions by determining their hypocotyl length, with *phyA-211* and *phyB-9* mutants as controls. Fluence rate–response curve analyses showed that *arf2-6* displayed more elongated hypocotyls compared with wild-type seedlings at almost all of the fluence rates of Rc and FRc used (Figure 6c). When grown under high Rc, *arf2-6* hypocotyls showed significant elongation compared with the wild-type control (Figure 6c), suggesting the *arf2-6* mutation strongly confers

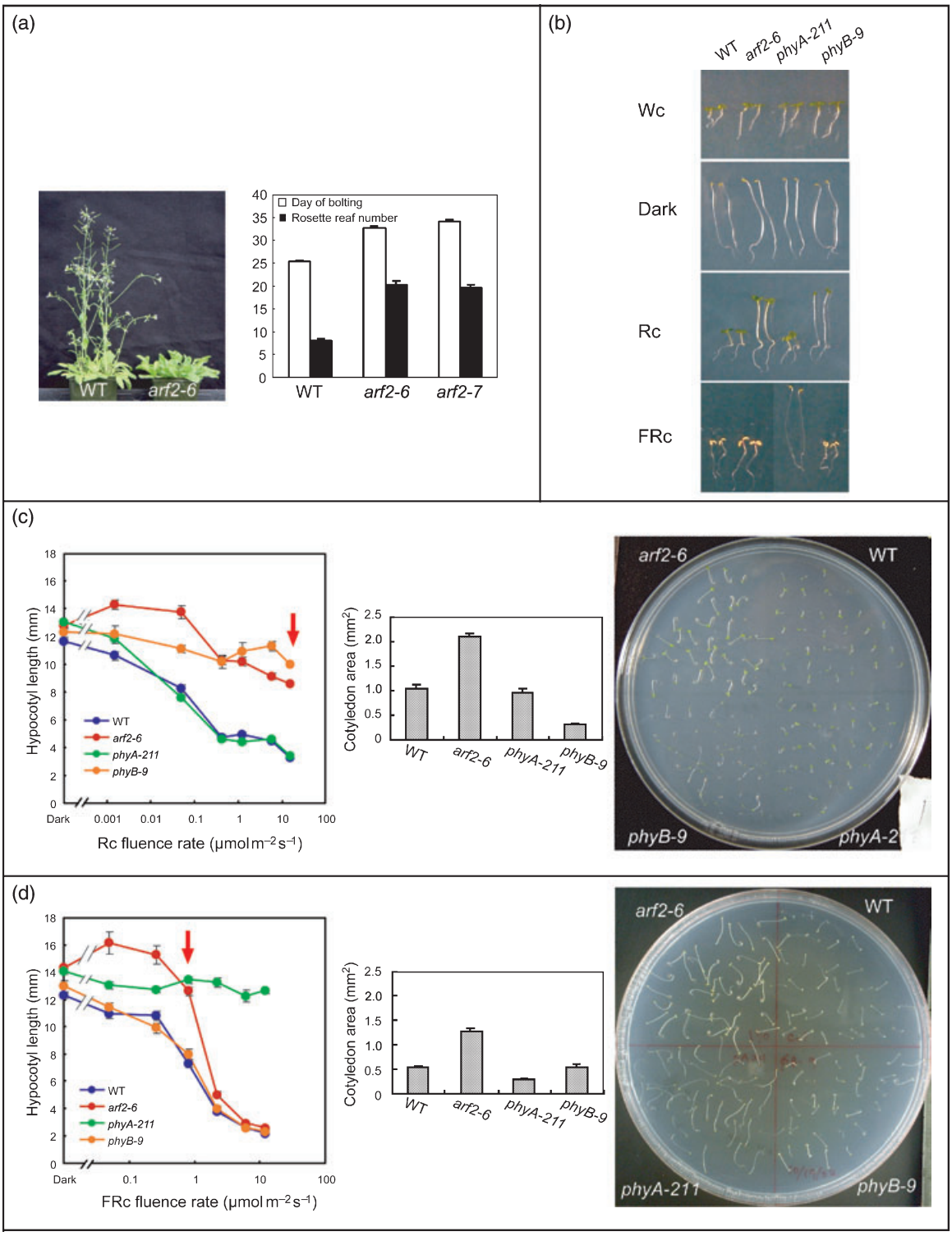

hyposensitivity under Rc conditions compared with FRc. However, *arf2-6* seedlings also displayed slightly longer hypocotyls compared with wild-type seedlings even when grown under dark conditions (Figure 6c,d). Roots of *arf2-6* mutant seedlings are also more elongated compared with the wild type, under all light conditions (Figure 6b; data not shown).

Unlike other typical light sensing-defective mutants, such as *phyA-211* and *phyB-9*, *arf2-6* mutant seedlings have significantly enlarged cotyledons under both Rc and FRc conditions despite more elongated hypocotyls (Figure 6c,d). Furthermore, *arf2-6* seedlings have increased levels of anthocyanin content when grown in FRc (data not shown). In addition, hypocotyls of *arf2-6* seedlings are thicker than wild type whereas *phyA-211* (grown under FRc) and *phyB-9* (grown under Rc) have thin hypocotyls like etiolated seedlings (Figure 6c,d; data not shown). Similar seedling phenotypes under various light conditions were also observed in *arf2-7* and *arf2-8* (Figure 8; data not shown). P_{35S}*:ARF2* plants showed long and thick hypocotyl and large cotyledon phenotypes under Rc and FRc in their seedling stage (Figure 7a,b). The behavior of the cosuppressed line was similar to that of the *arf2-6* mutant under various Rc and FRc conditions (compare Figure 7c,d with Figure 6c,d). These observations suggest that *ARF2* may participate in growth regulation of hypocotyl and cotyledon development in both light- and dark-grown seedlings rather than directly regulate light signaling pathway(s). Figure 8 shows the morphological comparison of seedling phenotypes of the *arf2* mutants and the P_{35S}*:ARF2* transgenic line with those of wild type. As described above, all *arf2* T-DNA insertion mutants (*arf2-6*, *arf2-7* and *arf2-8*) exhibited longer hypocotyls and roots and enlarged cotyledons under both FRc and Rc conditions. In addition, the *arf2* T-DNA mutants and P_{35S}*:ARF2* seedlings showed longer hypocotyls and enlarged cotyledons in the dark as well (Figure 8). Especially, P_{35S}*:ARF2* seedlings displayed significantly more elongated hypocotyls than the other genotypes.

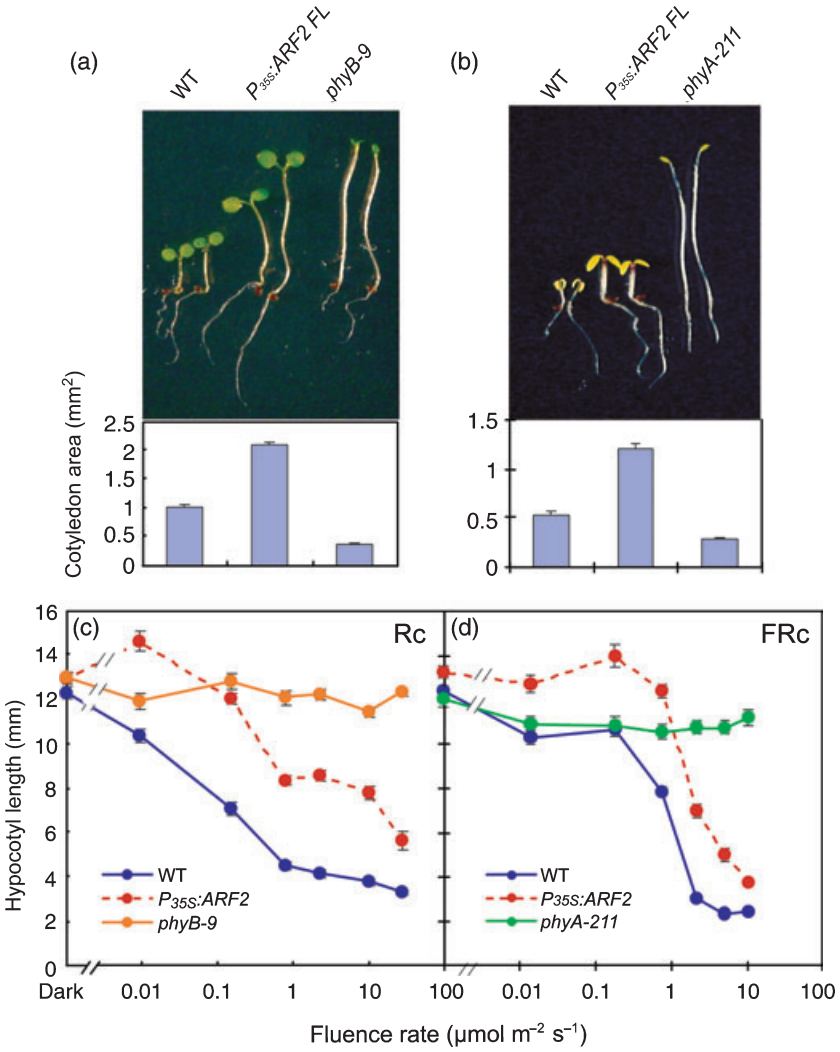

Figure 7. Light-related phenotype of Pro_{35s}*:ARF2* transgenic seedlings. Top left: phenotype of wild type (WT), Pro_{35s}*:ARF2* and *phyB-9* seedlings grown for 4 days under Rc (27 μmol m^{-2} sec^{-1}). Cotyledon area of different genotypes shown above is also represented. Top right: phenotype of WT, Pro_{35s}*:ARF2* and *phyA-211* seedlings grown for 4 days under FRc (10.53 μmol m^{-2} sec^{-1}). Cotyledon area of different genotypes shown above is also represented. Bottom: Rc and FRc fluence rate–response curves for hypocotyl length in WT, Pro_{35s}*:ARF2* and *phyB-9*/or *phyA-211* seedlings. Hypocotyl length and cotyledon area are expressed as the average of more than 25 seedlings. Bars represent SE of the average.

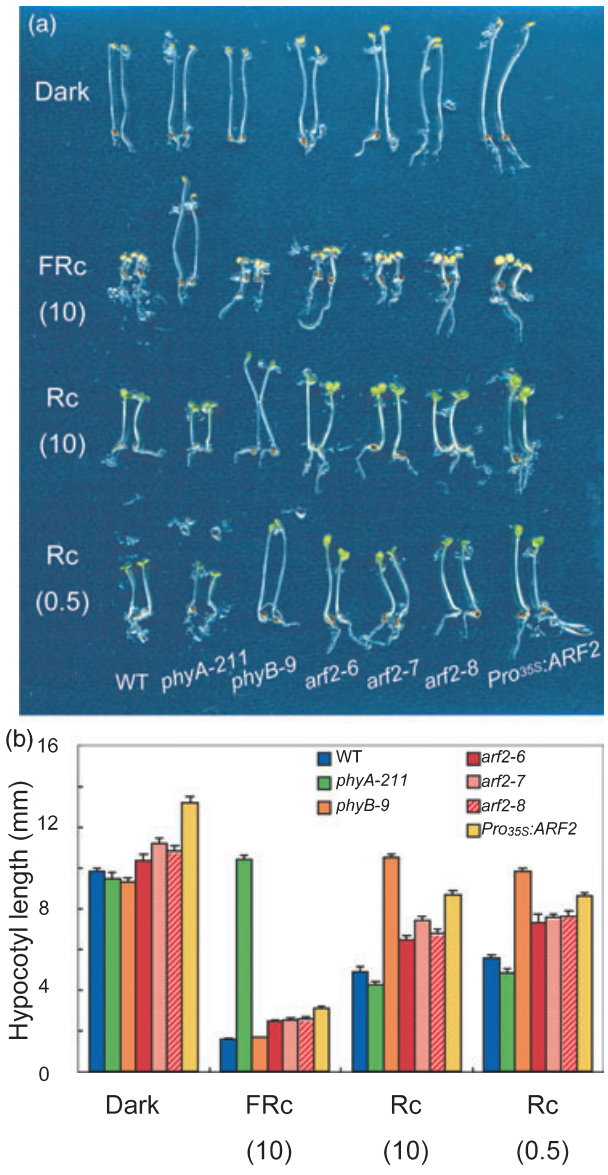

Figure 8. Growth of *arf2* mutants in the dark.
(a) Morphological comparison of the *arf2* T-DNA insertion mutants and the Pro_{35s}*:ARF2* seedlings. Wild type (WT), *phyA-211*, *phyB-9*, *arf2-6*, *arf2-7*, *arf2-8* and Pro_{35s}*:ARF2* seedlings were grown for 4 days under dark (dark), 10 μmol m^{-2} sec^{-1} FRc (FRc 10), 10 μmol m^{-2} sec^{-1} Rc (Rc 10) or 0.5 μmol m^{-2} sec^{-1} Rc (Rc 0.5).
(b) Quantitative analysis of the results shown in (a). Forty seedlings were used per measurement.

Microarray analysis

In order to determine the effects of the *arf2-6* mutation on global auxin-regulated gene expression, we conducted hybridization experiments with Affymetrix microarrays (Affymetrix ATH1 GeneChip) using RNA from control and IAA (5 μM) -treated wild type and *arf2-6* 7-day old, light-grown seedlings. Triplicate samples from each treatment were analyzed as previously described (Okushima *et al.*, 2005) and the data demonstrated that the mutation did not affect auxin-regulated gene expression (Figure 9).

Discussion

ARF2 *and plant growth*

Plant growth is regulated by coordinated cell division and expansion (Collett *et al.*, 2000). The *arf2* mutants exhibit pleiotropic effects, including larger plant size and abnormal flower morphology. Similarly, Pro_{ARF2}*:GUS* is abundantly expressed in the site of altered morphology in *arf2* mutants. However, in etiolated seedlings, there is a discrepancy between the expression patterns of Pro_{ARF2}*:GUS* observed in this study and Pro_{ARF2}*:GUS:ARF2*, reported by Li *et al.* (2004). Pro_{ARF2}*:GUS:ARF2* is expressed in the cotyledon, but is not expressed in the hypocotyls; whereas Pro_{ARF2}*:GUS* is strongly expressed in the apical portion of the hypocotyls and is not expressed in cotyledons. This difference may be due to post-transcriptional regulation of the Pro_{ARF2}*:GUS:ARF2* transcript.

The *arf2* mutants have a long hypocotyl phenotype under a wide range of Rc and FRc fluence conditions. They also have elongated hypocotyls in the dark and under continuous blue light (data not shown). As auxin has a central role in hypocotyl elongation, it may be suggested that the elongated hypocotyl phenotype of the *arf2* mutants is caused by increased auxin content or an alteration in auxin sensing. Many of the mutants with altered auxin sensitivity or content exhibit phenotypes associated with their hypocotyl length supporting this hypothesis. For example, several *Aux/IAA* gain-of-function mutants such as *axr2*/iaa7, axr3/*iaa17*, *shy2*/*iaa3* and *axr1* have short hypocotyls (Collett *et al.*, 2000; Jensen *et al.*, 1998; Leyser *et al.*, 1993; Reed, 2001; Rouse *et al.*, 1998). Plants with decreased free IAA content such as 35S-iaaL (Jensen *et al.*, 1998) and *cyp79B2 cyp79B3* (Zhao *et al.*, 2002) have shorter hypocotyls compared with the wild type under light conditions. However, increased free auxin content has opposite effects on hypocotyl elongation. Mutations in the *SUR1/RTY/ALF1* and *SUR2/CYP83B1/RED1* loci and overexpression of *YUCCA* and *CYP79B2* genes result in elongated hypocotyl phenotypes (Barlier *et al.*, 2000; Delarue *et al.*, 1998; Hoecker *et al.*, 2004; Zhao *et al.*, 2001, 2002). Finally, *19S-iaaM* transgenic lines which overexpress the bacterial Trp monooxygenase, have enhanced free auxin levels and their hypocotyls are longer than the wild type (Romano *et al.*, 1995).

A long hypocotyl phenotype was recently reported to be associated with the *arf8-1* mutant (Tian *et al.*, 2004). Mutant seedlings have a long hypocotyl phenotype in white, blue, and red or far-red light conditions. Their hypocotyl length is normal in the dark (Tian *et al.*, 2004). Overexpression of *ARF8* (*ARF8 OX*) results in a short hypocotyl phenotype and

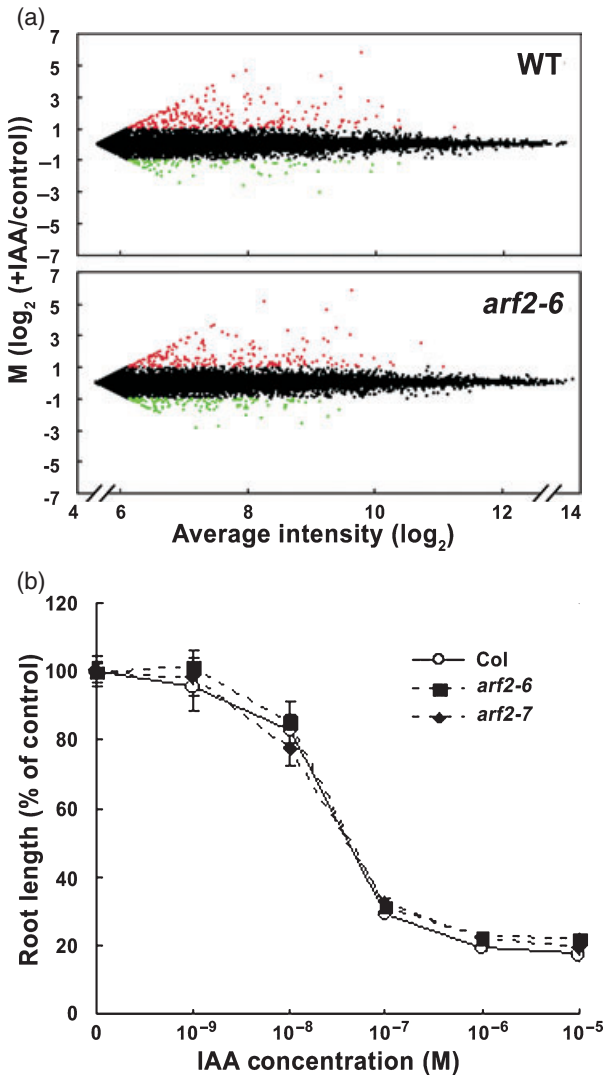

Figure 9. Global gene expression profiling and effect of auxin on root growth.
(a) MA plots (Dudiot *et al.*, 2002) showing changes of auxin-regulated gene expression levels in the wild type (WT) and arf2-6. Each plot represents the log ratio of the average of the auxin-treated samples (I) to the control samples (C) [M 1/4 log 2(I/C)] versus overall average intensity [A 1/4 log 2p(I × C)]. The genes induced by auxin treatment (M > 1) are highlighted in red, and the genes repressed by auxin treatment (M < 1) are highlighted in green. The data were further analyzed for variance to extract statistically valid auxin-regulated genes (see Okushima *et al.*, 2005).
(b) Inhibition of root growth by exogenous auxin. Each value represents the average of more than 10 seedlings. Bars represent SE of the average.

the free IAA content was reduced. Lateral root formation was also correlated with free auxin levels. The authors attributed the hypocotyl phenotypes to be the result of alteration in auxin homeostasis brought about by changes in gene expression of GH3 gene family members (Staswick *et al.*, 2002, 2005; Tian *et al.*, 2004).

Although *arf2* mutants show long hypocotyl phenotype under various light conditions, the phenotype of *arf2* differs from that of plants with altered auxin level (discussed above) or defective in phytochrome and cryptochrome signaling. The most striking difference between *arf2* and other long hypocotyl mutants is their cotyledon phenotype. Both under light and dark conditions, *arf2* seedlings have cotyledons that are larger than other mutants or transgenic plants mentioned above. Mutants with increased free auxin content [overexpressors of *YUCCA* and *CYP79B2* (Zhao *et al.*, 2001, 2002), *sur1/alf1* (Boerjan *et al.*, 1995), *sur2/cyp83B1/red1* (Hoecker *et al.*, 2004)], and mutants defective in phytochrome or cryptochrome signaling have small cotyledons (Cashmore *et al.*, 1999; Quail, 2002). In addition, unlike *arf8-1*, the *arf2* mutants do not show any phenotypes in common with the auxin perception-defective mutants. Root growth of *arf2* seedlings is inhibited by exogenous IAA application (Figure 9b), and they have the same numbers of lateral roots as the wild type (data not shown). In addition, both *arf2-6* and *arf2-7* mutant seedlings exhibit normal tropic responses (data not shown). A striking phenotypic difference between *arf2* and other long hypocotyl mutants, in addition to cotyledon size, is the radial swelling of hypocotyl and inflorescence stems, reminiscent of one of the 'triple response' characteristics (Guzman and Ecker, 1990).

Global gene expression profiling of liquid-cultured *arf2-6* seedlings is almost the same as that of the wild-type seedling treated with or without 5 μM IAA for 2 h. The *arf2* mutation did not affect the auxin-induced or -repressed genes, including *Aux/IAAs* and *GH3* gene family members (data not shown). Furthermore, these data suggest that the *arf2* mutation does not affect auxin signaling or the endogenous free auxin content. More importantly, the data suggest that ARF2 does not participate in the auxin response pathway in 7-day-old, light-grown Arabidopsis seedlings.

ARF2 *and senescence*

The adult phenotypes of *arf2* and ethylene-insensitive mutants share several similarities. Delayed floral organ abscission is observed in several ethylene response mutants such as *ethylene insensitive2* (*ein2*), *ein3* and *ethylene-resistant1* (*etr1*) (Bleecker and Patterson, 1997; Butenko *et al.*, 2003; Chao *et al.*, 1997; Patterson, 2001). The *ein2* and the *etr1* mutant also have larger rosette leaf size, slightly delayed flowering time compared with the wild type, and delayed leaf senescence (Guzman and Ecker, 1990; Mizukami, 2001; Oh *et al.*, 1997). These similarities between ethylene-insensitive and *arf2* mutants suggest that components of ethylene biosynthesis or perception may be defective in the *arf2* mutants. Furthermore, it is well established that pollination causes a rapid increase in ethylene production, first in the gynoecium and subsequently in the petals (Davies, 1995; Tang and Woodson, 1996; Tang *et al.*, 1994). Members of the *ACS* and *ACO* gene families are induced rapidly after pollination in carnation and tomato flowers

(Jones and Woodson, 1997; Llop-Tous *et al.*, 2000). We also observed accumulation of *ACS2* and *ACS8* transcripts after anthesis, suggesting that these genes may be involved in flower senescence (Figure 4c). Several *ACS*s including *ACS2*, *ACS6* and *ACS8* are expressed in various flower organs (Tsuchisaka and Theologis, 2004). The expression of *ACS2*, *ACS6* and *ACS8* is impaired in the *arf2-6* mutant at the time of flowering (Figure 4d). We could not reliably determine ethylene production in wild type and *arf2* mutant flowers; however, we attribute the enhanced flower resistance to senescence to be due to the inhibition of ACS activity. The *ACS6* and *ACS8* genes are auxin-inducible (Tsuchisaka and Theologis, 2004; Yamagami *et al.*, 2003) and their approximately 2 kb promoter regions contain four and six *AuxREs*, respectively. We do not know whether the expression of these *ACS* gene family members is regulated by auxin via the ARF2-Aux/IAA signaling system (Dharmasiri and Estelle, 2004). The possibility exists that they are regulated by *ARF2* via a non-IAA signaling apparatus.

Etiolated *arf2* mutant seedlings do not show any defect in apical hook formation (Li *et al.*, 2004; data not shown). However, *arf1 arf2* double mutant seedlings show exaggerated apical hook formation (Li *et al.*, 2004). *ARF1* is a close relative of *ARF2*, and *arf1* single mutants fail to show any obvious phenotypes (Li *et al.*, 2004; Okushima *et al.*, 2005), suggesting that *ARF2* negatively regulates hook formation redundantly with *ARF1.* Li *et al.* (2004) were the first to report the central role of *ARF2* in ethylene- and light-mediated plant growth. They discovered that extragenic suppressors of the hookless phenotype (*hls1*; Lehman *et al.*, 1996) reside in the *ARF2* locus. *ARF2* acts downstream of *HLS1* and negatively regulates hook formation. ARF2 protein stability is regulated in an HLS1-dependent manner by the ethylene and the light signaling systems. HLS1 appears to function as a central integrator of ethylene, auxin and light signaling pathways in differential hypocotyl cell elongation (Li *et al.*, 2004) with ARF2 as a major participant.

ARF2 *phenotypes and gene dosage*

The inflorescence phenotype of the *arf2* mutants is semi-dominant. Semi-dominant phenotypes of *ARF* loss-of-function mutants have also been reported for the *arf7/nph4-1* and *arf8-1* mutants. The *arf7/nph4-1* allele is considered a null, but it is semi-dominant with respect to phototropism (Stowe-Evans *et al.*, 1998). *ARF8*/*arf8-1* heterozygote seedlings show slightly longer hypocotyls than wild type (Tian *et al.*, 2004). Also, the *arf7*/*arf7*, *ARF19*/*arf19* and *ARF7*/*arf7 arf19*/*arf19* seedlings display significantly decreased numbers of lateral roots compared with the *arf7* or *arf19* single mutants (Y. Okushima, unpublished data). In addition, several of the phenotypes exhibited by the *arf2* alleles behave in both a recessive (flower morphology) and semi-dominant (inflorescence length and thickness) manner. These data suggest a regulatory role for the ARF2 protein level in various cells and tissues in exerting its molecular and developmental function(s).

Role of ARF2 *in auxin signaling*

Mutations in other *ARF* gene family members such as *arf3*/*ettin*, *arf5/mp* and *arf7/nph4* also exhibit visible and obvious phenotypes during plant growth and development and their developmental defects appear to be associated with altered auxin response or auxin distribution (Hardtke and Berleth, 1998; Harper *et al.*, 2000; Sessions *et al.*, 1997). In contrast, the phenotypes of *arf2* mutants do not appear to be caused by direct effect on auxin signaling (see above). ARF2 is thought to function as a transcriptional repressor by binding to synthetic auxin response elements (Tiwari *et al.*, 2003; Ulmasov *et al.*, 1999a). The prospect arises that its pleiotropic effects may be mediated by negatively modulating the transcription of developmental genes that are involved in cell proliferation and organ growth. Global gene expression analysis (microarray analysis) and root auxin sensitivity assays failed to detect significantly altered auxin responses in the *arf2* mutants. Furthermore, *DR5: GUS* gene expression in *arf2-3* is similar to that observed in the wild type, but the *arf2-3* mutation partially restores *DR5: GUS* expression within the cells located on the concave side of the hook in the *arf2-3 hls1-1* double mutant in the presence of ethylene, suggesting that ARF2 functions as a negative regulator of differential auxin response (Li *et al.*, 2004).

ARF2 was originally identified as an ARF1 binding protein, forming heterodimers with ARF1 in a yeast two-hybrid system (Ulmasov *et al.*, 1997a). The role of ARF2 protein in auxin signaling is still largely unknown. ARF2 may titrate the activity of other ARF transcriptional activators by heterodimerization. However, both ARF5 and ARF7 transcriptional activators fail to interact or interact only very weakly with ARF transcriptional repressors including ARF1 and ARF2 (Hardtke *et al.*, 2004). Furthermore, ARF1 and ARF2 do not interact with IAA17 in carrot cells, raising the prospect that the ARF transcriptional repressors may not be targeted by all the Aux/IAA proteins (Tiwari *et al.*, 2003). Considering the strong binding activity of ARF2 to synthetic auxin response elements (Ulmasov *et al.*, 1999a), ARF2 may mask *AuxRE*s, thereby preventing the binding of other ARFs, especially ARF transcriptional activators. Considering the ubiquity of the *AuxRE* sequence (TGTCTC) throughout the Arabidopsis genome, ARF2 may also bind to the promoter region of genes not directly regulated by auxin or genes not directly participating in auxin signaling. Alternatively, the ARF2 protein may titrate or regulate other unidentified factors by protein–protein interaction. It is of great interest that the N-terminal region (upstream to DBD) of ARF2 is unique among all other ARF gene family members. This region has a small sequence similar to the active phytochrome binding

(APB) domain, which is found in the N-terminal region of the bHLH members that can bind to the Pfr form of PHYB (Khanna *et al.*, 2004). Whether ARF2 interacts with the various phytochromes via its APB-like domain in its N-terminus is an important issue, worthy of further investigation. Global genomic approaches have the potential to unmask the vast heterodimerization potential among members of the *ARF* and *AUX/IAA* gene families in *vitro* and *in planta*. The molecular visualization and functional elucidation of this potential is the 'Rosetta stone' of auxin action.

In conclusion, we have presented the partial morphological and molecular characterization of three T-DNA insertion mutants in the *ARF2* locus of the Arabidopsis genome that cause pleiotropic developmental defects. The phenotypes described herein and by Li *et al.* (2004) suggest that the ARF2 transcription factor acts as a positive activator of flowering senescence and abscission and as a repressor of cell growth in the presence or absence of light, and differential hypocotyl growth (hook formation). The findings presented herein also raise the question whether all *ARF* gene family members and their splice variants (Okushima *et al.*, 2005) participate in the AUX/IAA-ARF auxin signaling apparatus throughout the plant life cycle (Dharmasiri and Estelle, 2004).

Experimental procedures

Materials

The *pBI101* vector was purchased from Clontech (Palo Alto, CA, USA). All chemicals used for this study were American Chemical Society (ACS) reagent grade or molecular biology grade. Oligonucleotides were purchased from Operon Technologies, Inc. (Alameda, CA, USA), or synthesized in house with a Polyplex Oligonucleotide Synthesizer (GeneMachines, Inc., San Carlos, CA, USA).

Molecular biology

Standard protocols were followed for DNA manipulations described in Sambrook *et al.* (1989). Standard protocols for DNA sequencing were used to confirm the accuracy of the DNA constructs.

Plant growth conditions

Arabidopsis thaliana ecotype Columbia (Col) was used throughout this study. The *ARF2* T-DNA insertion mutant alleles, *arf2-6*, *arf2-7* and *arf2-8*, were those isolated by Okushima *et al.* (2005). Seeds were surface-sterilized for 8 min in 5% sodium hypochlorite + 0.15% Tween 20, excessively rinsed in distilled water and plated on 0.8% agar plates (select agar; Life Technologies, Inc., Rockville, MD, USA) containing 0.5X Murashige-Skoog salts (Life Technologies, Inc.) + 0.5 mM MES, pH 5.7 + 1% sucrose + 1 X vitamin B5. The plates were incubated in the dark at 4°C for 2 days and were subsequently transferred to a 16 h light/8 h dark cycle at 22°C for 10 days. Subsequently, the seedlings were transplanted to soil and were grown on 16 h light/8 h dark cycle at 22°C to obtain mature plants. The auxin sensitivity assay (effect of auxin on root growth) was performed as follows: 4-day-old, light-grown seedlings were transferred to vertically oriented agar plates containing appropriate concentrations of IAA. Root length was determined after an additional 5 days of growth using the NIH Image 1.63 program (http://rsb.info.nih.gov/nih-image/download.html). Flowering time is expressed in number of days from germination to bolting. Plants were considered to have bolted when the length of inflorescence grew approximately 1 cm. Average bolting times were calculated from at least 12 plants of each line.

Red/far-red light experiments

Light experiments were performed as previously described (Huq *et al.*, 2000). Seed were sterilized and plated on 0.5X MS agar medium without sucrose. The plates were kept in the dark at 4°C for 4 days. After an initial 3 h of continuous white light treatment, plates were transferred to the dark for 21 h at 21°C and then transferred to Rc or Frc light conditions. They were kept there for 3 days at 21°C. The plates with control dark-grown seedlings were kept in the dark. The light sources used in this study have been described (Wagner *et al.*, 1991). Fluence rate of the various lights was measured by a spectroradiometer (model LI-1800; LiCor, Lincoln, NE, USA). The hypocotyl length and cotyledon area of at least 25 seedlings were measured using a digital camera and the NIH Image 1.63 program. *phyA-211* (Reed *et al.*, 1994) and *phyB-9* (Reed *et al.*, 1993) null PhyA and PhyB mutants were used as controls.

Construction of ARF2 *promoter-GUS transgenic lines*

A 2 kb *ARF2* promoter fragment upstream of the translation initiation codon was synthesized by PCR using wild type (Col) genomic DNA with the following primers: F: 5′-CGTCGACGGAATGGCCGAATTACAG-3′; R: 5′-AAGGATCCATACCTTCCGAAGCTCAGATCTG-3′.

The underlined sequences (non-native sequences) represent the *Sal*I and *Bam*HI cloning restriction sites, respectively. The PCR product was subcloned into *pPCR-script Amp SK (+)* (Stratagene, La Jolla, CA, USA) and its sequence was confirmed. The 2.0 kb *Sal*I-*Bam*HI fragment was subcloned into the *Sal*I-*Bam*HI sites of the *pBI101.2* binary vector (Clontech) giving rise to Pro_{ARF2}: *GUS*. The construct was introduced into *Agrobacterium tumefaciens* strain GV3101 (MP90) by electroporation, and wild type Col plants were transformed using the floral dip method (Clough and Bent, 1998). T_1 seeds were selected on medium containing 50 μg ml^{-1} kanamycin and 100 μg ml^{-1} carbenicillin and resistant seedlings were transferred to soil. GUS expression was examined by incubating tissue from T_2 or T_3 plants in 50 mM sodium phosphate buffer (pH 7.0) containing 0.4 mg ml^{-1} 5-bromo-4-chloro-3-indolyl-β-D-glucuronic acid (X-Gluc), 1 mM potassium ferricyanide, 1 mM potassium ferrocyanide and 0.5 % Triton X-100 for 5 h at 37°C, followed by incubation in 70% ethanol to remove chlorophyll (Jefferson *et al.*, 1987). Photographs were taken with a SPOT digital camera using a dissecting microscope.

ARF2 *overexpression and RNAi transgenic lines*

Transgenic plants overexpressing the *ARF2* mRNA (Pro_{35S}*: ARF2)* under the control of the *35S* promoter was generated by subcloning an error-free *ARF2* ORF (Okushima *et al.*, 2005) as a *Cla*I/*Xho*I fragment into the binary vector *pKF111. XL* (Ni *et al.*, 1998) and transforming plants as described by Clough and Bent (1998). To silence *ARF2* gene expression by double-stranded RNAi, we used the

pHANNIBAL vector which can be used to generate intron-containing hairpin loop RNA (ihpRNA) (Wesley *et al.*, 2001). An *ARF2* cDNA fragment was ligated in the sense and antisense orientation into *pHANNIBAL* (Wesley *et al.*, 2001).

The cDNA fragments were amplified using two primer pairs. Fragment A-Sense, was introduced as a *Xho*I-*Sac*I fragment; nucleotides 1201–2249 are underlined. F: 5′-GCCTCGAGTCCTG-TTCCAATGCCTAGG-3′ and R: 5′-AGGAGCTCTGAACGGCCAAGT-GCAATTCC-3′. Fragment B-Antisense, was introduced as a *Bam*HI-*Cla*I fragment; nucleotides 1206–2251 are underlined. F: 5′-GCG-GATCCTCCTGTTCCAATGCCTAGG-3′ and F: 5′-TGATCGATCCACT-GAACGGCCAAG-3′.

Fragment A was subcloned as *Xho*I-*Sac*I (blunt) fragment into the *Xho*I-*kpn*I (blunt) sites of *pHANNIBAL*. Fragment B was subcloned as a *BamH*I/*Cla*I fragment into the *BamH*I-*Cla*I sites of *pHANNIBAL*. The *ARF2* ihpRNA construct was subcloned as NotI fragment into the binary vector *pART27* (Wesley *et al.*, 2001) and plants were transformed as described by Clough and Bent (1998). T_1 transformants were selected on plates containing 10 μg ml^{-1} ammonium glufosinate and 100 μg ml^{-1} carbenicillin (*Pro*$_{35S}$*: ARF2*) or 50 μg ml^{-1} kanamycin and 100 μg ml^{-1} carbenicillin (*ARF2 RNAi*), and resistant seedlings were transferred to soil. Transgenic lines with single insertion were selected by examining the ammonium glufosinate (*Pro*$_{35S}$*: ARF2*) or kanamycin (*ARF2 RNAi*) resistance segregation ratio of T_2 seedlings. Homozygous lines were identified in T_3 generation and T_3 homozygous lines were used for phenotypic analysis.

RT-PCR and RNA hybridization analyses

Expression of *ARF2* mRNA in the *arf2-6*, *-7*, *-8* insertion alleles, *Pro*$_{35S}$*: ARF2* and *RNAi* lines was monitored by RT-PCR. Total RNA was extracted from 7-day-old, light-grown seedlings using the RNAqueous RNA isolation kit with Plant RNA isolation aid (Ambion Inc., Austin, TX, USA). Total RNA (1.1 μg) was treated with RQ1 RNase-free DNase (Promega, Madison, WI, USA) and first strand cDNA was synthesized using an oligo$(dT)_{12-18}$ primer or random primers and SuperScript II reverse transcriptase (Invitrogen, Carlsbad, CA, USA).

One-hundredth of the resulting cDNA was subjected to 31 cycles of amplification using *ARF2*-specific primers: ARF2-F1 5′-GCGAGTTCGGAGGTTTCAATGAAA-3′ (location 4–27 nt); ARF2-R1 5′-TCTGTAAAGAGCAGCCTCAGGGTCC-3′ (location 156–180 nt).

The amplification conditions were initial denaturation at 94°C/5 min; 31 cycles at 94°C/30 sec; 60°C/30 sec; 72°C/40 sec; and final elongation 72°C/7 min.

For Northern blot analysis, total RNA was extracted from 7-day-old, light-grown seedlings using RNAqueous RNA isolation kit with Plant RNA isolation aid (Ambion). Twenty micrograms of total RNA was fractionated by electrophoresis on 1.2% agarose gels containing 2.2 M formaldehyde and 1X MOPS [3-(N-morpholino) propanesulfonic acid] buffer, and blotted onto nylon Hybond N membrane (Amersham-Pharmacia Biotech, Piscataway, NJ, USA). After cross linking the RNA by UV irradiation, hybridization was carried out at 42°C for 16 h in hybridization buffer containing ^{32}P-labeled *ARF2* cDNA probe, 50% formamide, 10% dextran sulfate, 1X Denhardt's solution (0.02% Ficoll 400, 0.02% polyvinylpyrrolidone and 0.02% BSA), 0.5% SDS, 3X SSC and 50 mM Tris-HCl (pH 7.5). The membrane was washed three times with 0.2X SSC containing 0.1% SDS at 65°C. The expression levels were determined with a Storm 860 PhosphorImager (Molecular Dynamics, Sunnyvale, CA, USA).

Expression of the *ACS* genes (Yamagami *et al.*, 2003) during flower and silique development was determined by RT-PCR analysis. Tissue samples were collected from seven developmental stages depending on morphological appearance. Stage 1: flower buds (stages 1–12); stage 2: flowers with anthesis (stages 13 and 14); stage 3: flowers with stigma extends above long stamen and petals – petals and sepals withering (stages 14 and 15); stage 4: all organs fall from siliques – immature siliques length with <5 mm (stage 17A); stage 5: immature siliques with 5–12 mm length (stage 17A); stage 6: immature siliques with 12–15 mm length, not getting thick yet (stage 17A); and stage 7: silique reaches its final length, getting thick already (stage 17B). The corresponding stages of flower development (shown in parenthesis) are those defined by Ferrandiz *et al.* (1999). Total RNA was isolated from various stages of flower and silique samples using RNAqueous RNA isolation kit with Plant RNA isolation aid (Ambion). For each sample, 2.5 μg of total RNA was treated with RQ1 RNase-free DNase (Promega) to eliminate genomic DNA contamination. First strand cDNA was synthesized with oligo$(dT)_{24}$ primers using a SuperScript II reverse transcriptase (Invitrogen). One-hundredth of the resulting cDNA was subjected to 30 (*ARF2*), 35 (*ACS* genes) or 25 (control *ACT8* gene) cycles of PCR amplification (95°C for 20 sec, 62°C for 20 sec, 72°C for 45 sec). The primers used for each *ACS* genes were previously described (Yamagami *et al.*, 2003). *ACT8* gene-specific primers described by An *et al.* (1996) were used for control amplification.

Immunoblot analysis

The level of ARF2 protein expression in the various mutants and transgenic lines was assessed by immunoblotting. We homogenized a tenth of a gram of 7-day-old, light-grown seedlings in 500 μl of SDS loading buffer: 250 mM Tris-HCl, 10% SDS, 25% glycerol, 0.1% bromophenol blue, 10% β-mercaptoethanol (Li *et al.*, 2004) and heated at 75°C for 15 min, and then the supernatants were collected by centrifugation; 15 μl was analyzed by SDS-PAGE (Weber *et al.*, 1972) and immunoblotting (Towbin *et al.*, 1979). Immunoblots were probed with a 1:1000 dilution of ARF2 antibody. The antibody–antigen complex was visualized using the ECL Western blotting analysis system (Amersham-Pharmacia Biotech) and exposure on Kodak BioMax XAR film (Kodak, Rochester, NY, USA).

Microarray analysis

Microarray experiments and data analysis were performed exactly as previously described (Okushima *et al.*, 2005). The entire data set has been deposited in the Gene Expression Omnibus database (http://www.ncbi.nlm.nih.gov/geo/) with accession numbers GSE631, GSM9620 and GSM9624–GSM9634.

Acknowledgements

We thank Dr Peter Quail for providing *phyA-211* and *phyB-9* seeds, allowing us to use his laboratory equipment for light experiments and for useful discussions; Dr Rajinish Khanna (PGEC) and Dr Enamul Huq (University of Texas) for their assistance and advice with the light-related experiments; Dr Hai Li (Ecker Lab, Salk) for providing antibody to the ARF2 protein; Dr Atsunari Tsuchisaka (PGEC) for providing PCR primers of the *ACS* genes and Dr Peter Waterhouse (CSIRO) for providing the RNAi vectors. The technical assistance of Ms Beth Hughes is greatly appreciated. The assistance of Mr David Hantz and Ms Julie Calfas for greenhouse work is acknowledged. This research was supported by the National Institutes of Health grant (RO1 GM035447) to A.T.

References

Abel, S. and Theologis, A. (1996) Early genes and auxin action. *Plant Physiol.* **111**, 9–17.

Abel, S., Oeller, P.W. and Theologis, A. (1994) Early auxin-induced genes encode short-lived nuclear proteins. *Proc. Natl Acad. Sci. USA*, **91**, 326–330.

Abel, S., Ballas, N., Wong, L.-M. and Theologis, A. (1996) DNA elements responsive to auxin. *BioEssays*, **18**, 647–654.

An, Y.Q., McDowell, J.M., Huang, S., McKinney, E.C., Chambliss, S. and Meagher, R.B. (1996) Strong, constitutive expression of the Arabidopsis ACT2/ACT8 actin subclass in vegetative tissues. *Plant J.* **10**, 107–121.

Arabidopsis Genome Initiative. (2000) Analysis of the genome sequence of the flowering plant *Arabidopsis thaliana*. *Nature*, **408**, 796–815.

Barlier, I., Kowalczyk, M., Marchant, A., Ljung, K., Bhalerao, R., Bennett, M., Sandberg, G. and Bellini, C. (2000) The SUR2 gene of *Arabidopsis thaliana* encodes the cytochrome P450 CYP83B1, a modulator of auxin homeostasis. *Proc. Natl Acad. Sci. USA*, **97**, 14819–14824.

Bleecker, A.B. and Patterson, S.E. (1997) Last exit: senescence, abscission, and meristem arrest in Arabidopsis. *Plant Cell*, **9**, 1169–1179.

Boerjan, W., Cervera, M.T., Delarue, M., Beeckman, T., Dewitte, W., Bellini, C., Caboche, M., Van Onckelen, H., Van Montagu, M. and Inze, D. (1995) Superroot, a recessive mutation in Arabidopsis, confers auxin overproduction. *Plant Cell*, **7**, 1405–1419.

Butenko, M.A., Patterson, S.E., Grini, P.E., Stenvik, G.E., Amundsen, S.S., Mandal, A. and Aalen, R.B. (2003) INFLORESCENCE DEFICIENT IN ABSCISSION controls floral organ abscission in Arabidopsis and identifies a novel family of putative ligands in plants. *Plant Cell*, **15**, 2296–2307.

Cashmore, A.R., Jarillo, J.A., Wu, Y.J. and Liu, D. (1999) Cryptochromes: blue light receptors for plants and animals. *Science*, **284**, 760–765.

Chao, Q., Rothenberg, M., Solano, R., Roman, G., Terzaghi, W. and Ecker, J.R. (1997) Activation of the ethylene gas response pathway in Arabidopsis by the nuclear protein ETHYLENE-INSENSITIVE3 and related proteins. *Cell*, **89**, 1133–1144.

Clough, S.J. and Bent, A.F. (1998) Floral dip: a simplified method for *Agrobacterium*-mediated transformation of *Arabidopsis thaliana*. *Plant J.* **16**, 735–743.

Collett, C.E., Harberd, N.P. and Leyser, O. (2000) Hormonal interactions in the control of Arabidopsis hypocotyl elongation. *Plant Physiol.* **124**, 553–562.

Davies, P.J. (1995) *Plant Hormones: Physiology, Biochemistry and Molecular Biology*, 2nd edn. Dordrecht, The Netherlands: Kluwer Academic Publishers.

Delarue, M., Prinsen, E., Onckelen, H.V., Caboche, M. and Bellini, C. (1998) Sur2 mutations of *Arabidopsis thaliana* define a new locus involved in the control of auxin homeostasis. *Plant J.* **14**, 603–611.

Dharmasiri, N. and Estelle, M. (2004) Auxin signaling and regulated protein degradation. *Trends Plant Sci.* **9**, 302–308.

Dudiot, S., Yang, Y.H., Callow, M.J., and Speed, T.P. (2002) Statistical methods for identifying differentially expressed genes in replicated cDNA microarray experiments. *Statistica Sinica*, **12**, 111–139.

Ferrandiz, C., Pelaz, S. and Yanofsky, M.F. (1999) Control of carpel and fruit development in Arabidopsis. *Annu. Rev. Biochem.* **68**, 321–354.

Fowler, S., Lee, K., Onouchi, H., Samach, A., Richardson, K., Morris, B., Coupland, G. and Putterill, J. (1999) GIGANTEA: a circadian clock-controlled gene that regulates photoperiodic flowering in Arabidopsis and encodes a protein with several possible membrane-spanning domains. *EMBO J.* **18**, 4679–4688.

Fukaki, H., Tameda, S., Masuda, H. and Tasaka, M. (2002) Lateral root formation is blocked by a gain-of-function mutation in the SOLITARY-ROOT/IAA14 gene of Arabidopsis. *Plant J.* **29**, 153–168.

Gray, W.M., Kepinski, S., Rouse, D., Leyser, O. and Estelle, M. (2001) Auxin regulates SCF(TIR1)-dependent degradation of AUX/IAA proteins. *Nature*, **414**, 271–276.

Guilfoyle, T.J. and Hagen, G. (2001) Auxin response factors. *J. Plant Growth Regul.* **20**, 281–291.

Guilfoyle, T., Hagen, G., Ulmasov, T. and Murfett, J. (1998) How does auxin turn on genes? *Plant Physiol.* **118**, 341–347.

Guzman, P. and Ecker, J.R. (1990) Exploiting the triple response of Arabidopsis to identify ethylene-related mutants. *Plant Cell*, **2**, 513–523.

Hardtke, C.S. and Berleth, T. (1998) The Arabidopsis gene MONOPTEROS encodes a transcription factor mediating embryo axis formation and vascular development. *EMBO J.* **17**, 1405–1411.

Hardtke, C.S., Ckurshumova, W., Vidaurre, D.P., Singh, S.A., Stamatiou, G., Tiwari, S.B., Hagen, G., Guilfoyle, T.J. and Berleth, T. (2004) Overlapping and non-redundant functions of the Arabidopsis auxin response factors MONOPTEROS and NONPHOTOTROPIC HYPOCOTYL 4. *Development*, **131**, 1089–1100.

Harper, R.M., Stowe-Evans, E.L., Luesse, D.R., Muto, H., Tatematsu, K., Watahiki, M.K., Yamamoto, K. and Liscum, E. (2000) The NPH4 locus encodes the auxin response factor ARF7, a conditional regulator of differential growth in aerial Arabidopsis tissue. *Plant Cell*, **12**, 757–770.

Hayama, R. and Coupland, G. (2004) The molecular basis of diversity in the photoperiodic flowering responses of Arabidopsis and rice. *Plant Physiol.* **135**, 677–684.

Hoecker, U., Toledo-Ortiz, G., Bender, J. and Quail, P.H. (2004) The photomorphogenesis-related mutant red1 is defective in CYP83B1, a red light-induced gene encoding a cytochrome P450 required for normal auxin homeostasis. *Planta*, **219**, 195–200.

Huq, E., Tepperman, J.M. and Quail, P.H. (2000) GIGANTEA is a nuclear protein involved in phytochrome signaling in Arabidopsis. *Proc. Natl Acad. Sci. USA*, **97**, 9789–9794.

Jefferson, R.A., Kavanagh, T.A., Bevan, M.V. (1987) GUS fusions:β-glucuronidase as a sensitive and versatile gene fusion marker in higher plants. *EMBO J*, **6**, 3901–3907.

Jensen, P.J., Hangarter, R.P. and Estelle, M. (1998) Auxin transport is required for hypocotyl elongation in light grown but not dark-grown Arabidopsis. *Plant Physiol.* **116**, 455–462.

Jones, M.L. and Woodson, W.R. (1997) Pollination-induced ethylene in carnation (role of stylar ethylene in corolla senescence). *Plant Physiol.* **115**, 205–212.

Khanna, R., Huq, E., Kikis, E.A., Al-Sady, B., Lanzatella, C. and Quail, P.H. (2004) A novel molecular recognition motif necessary for targeting photoactivated phytochrome signaling to specific basic helix-loop-helix transcription factors. *Plant Cell*, **16**, 3033–3044.

Kim, J., Harter, K. and Theologis, A. (1997) Protein-protein interactions among the Aux/IAA proteins. *Proc. Natl Acad. Sci. USA*, **94**, 11786–11791.

Koornneef, M., Hanhart, C., van LoenenMartinet, C. and de Vries, H.B. (1995) The effect of day length on the transition to flowering in phytochrome deficient, late flowering and double mutants of *Arabidopsis thaliana*. *Physiol. Plant.* **95**, 260–266.

Lehman, A., Black, R. and Ecker, R. (1996) HOOKLESS1, an ethylene response gene, is required for differential cell elongation in the *Arabidopsis* hypocotyls. *Cell*, **85**, 183–194.

Leyser, H.M., Lincoln, C.A., Timpte, C., Lammer, D., Turner, J. and Estelle, M. (1993) Arabidopsis auxin-resistance gene AXR1 encodes a protein related to ubiquitin-activating enzyme E1. *Nature*, **364**, 161–164.

Leyser, O. (2002) Molecular genetics of auxin signaling. *Annu. Rev. Plant Biol.* **53**, 377–398.

Li, H., Johnson, P., Stepanova, A., Alonso, J.M. and Ecker, J.R. (2004) Convergence of signaling pathways in the control of differential cell growth in Arabidopsis. *Dev. Cell*, **7**, 193–204.

Liscum, E. and Reed J.W. (2002) Genetics of Aux/IAA and ARF action in plant growth and development. *Plant Mol. Biol.* **49**, 387–400.

Llop-Tous, I., Barry, C.S. and Grierson, D. (2000) Regulation of ethylene biosynthesis in response to pollination in tomato flowers. *Plant Physiol.* **123**, 971–978.

Mizukami, Y. (2001) A matter of size: developmental control of organ size in plants. *Curr. Opin. Plant Biol.* **4**, 533–539.

Nagpal, P., Walker, L.M., Young, J.C., Sonawala, A., Timpte, C., Estelle, M. and Reed, J.W. (2000) AXR2 encodes a member of the Aux/IAA protein family. *Plant Physiol.* **123**, 563–573.

Nemhauser, J.L., Feldman, L.J. and Zambryski, P.C. (2000) Auxin and ETTIN in Arabidopsis gynoecium morphogenesis. *Development*, **127**, 3877–3888.

Ni, M., Tepperman, J.M. and Quail, P.H. (1998) PIF3, a phytochrome-interacting factor necessary for normal photo induced signal transduction, is a novel basic helix-loop-helix protein. *Cell*, **95**, 657–667.

Oh, S.A., Park, J.H., Lee, G.I., Paek, K.H., Park, S.K. and Nam, H.G. (1997) Identification of three genetic loci controlling leaf senescence in *Arabidopsis thaliana*. *Plant J.* **12**, 527–535.

Okushima, Y., Overvoorde, P.J., Arima, K. *et al.* (2005) Functional genomic analysis of the AUXIN RESPONSE FACTOR gene family members in *Arabidopsis thaliana*: unique and overlapping functions of ARF7 and ARF19. *Plant Cell*, **17**, 444–463.

Ouellet, F., Overvoorde, P.J. and Theologis, A. (2001) IAA17/AXR3: biochemical insight into an auxin mutant phenotype. *Plant Cell*, **13**, 829–841.

Patterson, S.E. (2001) Cutting loose. Abscission and dehiscence in Arabidopsis. *Plant Physiol.* **126**, 494–500.

Quail, P.H. (2002) Phytochrome photosensory signaling networks. *Nat. Rev. Mol. Cell Biol.* **3**, 85–93.

Ramos, J.A., Zenser, N., Leyser, O. and Callis, J. (2001) Rapid degradation of auxin/indole acetic acid proteins requires conserved amino acids of domain II and is proteosome dependent. *Plant Cell*, **13**, 2349–2360.

Reed, J.W. (2001) Roles and activities of Aux/IAA proteins in Arabidopsis. *Trends Plant Sci.* **6**, 420–425.

Reed, J.W., Nagpal, P., Poole, D.S., Furuya, M. and Chory, J. (1993) Mutations in the gene for the red/far-red light receptor phytochrome B alter cell elongation and physiological responses throughout Arabidopsis development. *Plant Cell*, **5**, 147–157.

Reed, J.W., Nagatani, A., Elich, T.D., Fagan, M. and Chory, J. (1994) Phytochrome A and phytochrome B have overlapping but distinct functions in Arabidopsis development. *Plant Physiol.* **104**, 1139–1149.

Rogg, L.E., Lasswell, J. and Bartel, B. (2001) A gain-of-function mutation in IAA28 suppresses lateral root development. *Plant Cell*, **13**, 465–480.

Romano, C.P., Robson, P.R., Smith, H., Estelle, M. and Klee, H. (1995) Transgene-mediated auxin overproduction in Arabidopsis: hypocotyl elongation phenotype and interactions with the hy6-1 hypocotyl elongation and axr1 auxin-resistant mutants. *Plant Mol. Biol.* **27**, 1071–1083.

Rouse, D., Mackay, P., Stirnberg, P., Estelle, M. and Leyser, O. (1998) Changes in auxin response from mutations in an AUX/IAA gene. *Science*, **279**, 1371–1373.

Sambrook, J., Fritsch, E.F., and Maniatis, T. (1989) *Molecular Cloning: A Laboratory Manual*. 2nd Edn. Cold Spring Harbor: Cold Spring Harbor Laboratory Press, Woodbury, NY, USA.

Sessions, A., Nemhauser, J.L., McColl, A., Roe, J.L., Feldmann, K.A. and Zambryski, P.C. (1997) ETTIN patterns the Arabidopsis floral meristem and reproductive organs. *Development*, **124**, 4481–4491.

Staswick, P.E., Tiryaki, I. and Rowe, M.L. (2002) Jasmonate response locus JAR1 and several related Arabidopsis genes encode enzymes of the firefly luciferase superfamily that show activity on jasmonic, salicylic, and indole-3-acetic acids in an assay for adenylation. *Plant Cell*, **14**, 1405–1415.

Staswick, P.E., Serban, B., Rowe, M., Tiryaki, I., Maldonado, M.T., Maldonado, M.C. and Suza, W. (2005) Characterization of an Arabidopsis enzyme family that conjugates amino acids to indole-3-acetic acid. *Plant Cell*, **17**, 616–627.

Stowe-Evans, E.L., Harper, R.M., Motchoulski, A.V. and Liscum, E. (1998) NPH4, a conditional modulator of auxin-dependent differential growth responses in Arabidopsis. *Plant Physiol.* **118**, 1265–1275.

Tang, X. and Woodson, W.R. (1996) Temporal and spatial expression of 1-aminocyclopropane-1-carboxylate oxidase mRNA following pollination of immature and mature petunia flowers. *Plant Physiol.* **112**, 503–511.

Tang, X., Gomes, A., Bhatia, A. and Woodson, W.R. (1994) Pistil-specific and ethylene-regulated expression of 1-aminocyclopropane-1-carboxylate oxidase genes in petunia flowers. *Plant Cell*, **6**, 1227–1239.

Tian, Q. and Reed, J.W. (1999) Control of auxin-regulated root development by the *Arabidopsis thaliana* SHY2/IAA3 gene. *Development*, **126**, 711–721.

Tian, C.E., Muto, H., Higuchi, K., Matamura, T., Tatematsu, K., Koshiba, T. and Yamamoto, K.T. (2004) Disruption and overexpression of auxin response factor 8 genes of Arabidopsis affect hypocotyl elongation and root growth habit, indicating its possible involvement in auxin homeostasis in light condition. *Plant J.* **40**, 333–343.

Tiwari, S.B., Hagen, G. and Guilfoyle, T. (2003) The roles of auxin response factor domains in auxin-responsive transcription. *Plant Cell*, **15**, 533–543.

Tiwari, S.B., Hagen, G. and Guilfoyle, T.J. (2004) Aux/IAA proteins contain a potent transcriptional repression domain. *Plant Cell*, **16**, 533–543.

Towbin, H., Staehelin, T. and Gordon J. (1979) Electrophoretic transfer of proteins from polyacrylamide gels to nitrocellulose sheets: procedure and some applications. *Proc. Natl Acad. Sci. USA*, **76**, 4350–4354.

Tsuchisaka, A. and Theologis, A. (2004) Unique and overlapping expression patterns among the Arabidopsis 1-amino-cyclopropane-1-carboxylate synthase gene family members. *Plant Physiol.* **136**, 2982–3000.

Ulmasov, T., Hagen, G. and Guilfoyle, T.J. (1997a) ARF1, a transcription factor that binds to auxin response elements. *Science*, **276**, 1865–1868.

Ulmasov, T., Murfett, J., Hagen, G. and Guilfoyle, T.J. (1997b) Aux/IAA proteins repress expression of reporter genes containing natural and highly active synthetic auxin response elements. *Plant Cell*, **9**, 1963–1971.

Ulmasov, T., Hagen, G. and Guilfoyle, T.J. (1999a) Dimerization and DNA binding of auxin response factors. *Plant J.* **19**, 309–319.

Ulmasov, T., Hagen, G. and Guilfoyle, T.J. (1999b) Activation and repression of transcription by auxin-response factors. *Proc. Natl Acad. Sci. USA*, **96**, 5844–5849.

Valverde, F., Mouradov, A., Soppe, W., Ravenscroft, D., Samach, A. and Coupland, G. (2004) Photoreceptor regulation of CONSTANS protein in photoperiodic flowering. *Science*, **303**, 1003–1006.

Wagner, D., Tepperman, J.M. and Quail, P.H. (1991) Overexpression of phytochrome B induces a short hypocotyl phenotype in transgenic Arabidopsis. *Plant Cell*, **3**, 1275–1288.

Watahiki, M.K. and Yamamoto, K.T. (1997) The massugu1 mutation of Arabidopsis identified with failure of auxin-induced growth curvature of hypocotyl confers auxin insensitivity to hypocotyl and leaf. *Plant Physiol.* **115**, 419–426.

Weber, K., Pringle, J.R. and Osborn, M. (1972) Measurement of molecular weights by electrophoresis on SDS-acrylamide gel. *Methods Enzymol.* **26**, 3–27.

Weijers, D. and Jurgens, G. (2004) Funneling auxin action: specificity in signal transduction. *Curr. Opin. Plant Biol.* **7**, 687–693.

Wesley, S.V., Helliwell, C.A., Smith, N.A. *et al.* (2001) Construct design for efficient, effective and high-throughput gene silencing in plants. *Plant J.* **27**, 581–590.

Yamagami, T., Tsuchisaka, A., Yamada, K., Haddon, W.F., Harden, L.A. and Theologis, A. (2003) Biochemical diversity among the 1-amino-cyclopropane-1-carboxylate synthase isozymes encoded by the Arabidopsis gene family. *J. Biol. Chem.* **278**, 49102–49112.

Yang, X., Lee, S., So, J.H., Dharmasiri, S., Dharmasiri, N., Ge, L., Jensen, C., Hangarter, R., Hobbie, L., and Estelle, M. (2004) The IAA1 protein is encoded by AXR5 and is a substrate of SCFTIR1. *Plant J*, **40**, 772–782.

Zhao, Y., Christensen, S.K., Fankhauser, C., Cashman, J.R., Cohen, J.D., Weigel, D. and Chory, J. (2001) A role for flavin monooxygenase-like enzymes in auxin biosynthesis. *Science*, **291**, 306–309.

Zhao, Y., Hull, A.K., Gupta, N.R., Goss, K.A., Alonso, J., Ecker, J.R., Normanly, J., Chory, J. and Celenza, J.L. (2002) Trp-dependent auxin biosynthesis in Arabidopsis: involvement of cytochrome P450s CYP79B2 and CYP79B3. *Genes Dev.* **16**, 3100–3112.